
BREAKING WAVE LOADS ON IMMERSED MEMBERS OF OFFSHORE STRUCTURES

*Prepared by W.S. Atkins Engineering Sciences
for the Department of Energy*



Offshore Technology Report

Department of Energy

BREAKING WAVE LOADS ON IMMERSED MEMBERS OF OFFSHORE STRUCTURES

Author
R.C.T. RAINEY
W.S. Atkins Engineering Sciences Limited
Woodcote Grove
Ashley Road
Epsom
Surrey KT18 5BW

London: HMSO

© Crown copyright 1991
First published 1991
ISBN 0 11 413316 6

This publication forms part of a series of reports to the Department of Energy of work which has been wholly or in part supported by funds provided by the Department. Neither the Department nor the contractors concerned assume any liability for the reports nor do they necessarily reflect the views or policy of the Department.

Results, including detailed evaluation and, where relevant, recommendations stemming from these research projects, are published in the OTH series of reports.

Background information and data arising from these research projects are published in the OTI series of reports.

HMSO Standing order service

Placing a standing order with HMSO BOOKS enables a customer to receive other titles in this series automatically as published. This saves the time, trouble and expense of placing individual orders and avoids the problem of knowing when to do so.

For details please write to HMSO BOOKS (PC 13A/1), Publications Centre, PO Box 276, London SW8 5DT quoting reference 12.01.025

The standing order service also enables customers to receive automatically as published all material of their choice which additionally saves extensive catalogue research. The scope and selectivity of the service has been extended by new techniques, and there are more than 3,500 classifications to choose from. A special leaflet describing the service in detail may be obtained on request.

CONTENTS

	<u>Page</u>
List of Figures	2
List of Tables	2
SUMMARY	3
1. INTRODUCTION	4
2. WATER VELOCITY AND ACCELERATION IN A BREAKING WAVE	6
2.1 Selection of appropriate wave, wave height and wave period	
2.2 Selection of appropriate time and location within wave	
2.3 Acceleration constituents at chosen point	
2.4 Extent of high-acceleration region	
3. DERIVATION OF WAVE LOADS: IMPROVING ON "MORISON'S EQUATION"	19
3.1 A general formula for the potential-flow load on a fixed cylinder in waves	
3.2 First special case: cylinder parallel to the wave crests	
3.3 Second special case: circular cylinder perpendicular to the wave crests	
4. RESULTS OF SAMPLE CALCULATIONS	23
4.1 Choice of cylinder orientations for analysis	
4.2 Potential-flow load	
4.3 Load from the original and modified Morison inertia term	
4.4 Load from the Morison drag term	
5. CONCLUSIONS	27
REFERENCES	

LIST OF FIGURES

1. Fluid velocity, local acceleration and total acceleration behind the vertical face of a breaking wave
2. Loads on a cylinder of one metre radius parallel to wave crests
3. Wave loads on one metre radius cylinders of various orientations

LIST OF TABLES

1. Wave particle position, velocity and acceleration, time = 4.825 secs
2. Wave particle position, velocity and acceleration, time = 5.245 secs
3. Wave particle position, velocity and acceleration, time = 5.665 secs
4. Wave particle position, velocity and acceleration, time = 6.093 secs
5. Wave particle position, velocity and acceleration, time = 6.512 secs
6. Horizontal fluid velocities at points behind face of breaking wave
7. Vertical fluid velocities at points behind face of breaking wave

SUMMARY

Recent developments in the theoretical study of breaking waves have shown conclusively that these waves have a region where fluid accelerations are an order of magnitude greater than previously thought.

This project investigates the implications of these high accelerations on the fluid loading on tubular members typical of jacket structures in shallow UK coastal waters where, it is acknowledged, breaking waves can occur.

Results from a recently published authoritative description of breaking waves are used to determine wave kinematics in a representative breaking wave.

The obtained fluid velocities and accelerations are used to calculate drag and inertial components of fluid loading on a tubular member when fully immersed, comparing the inertial component as derived by three methods as follows:

- a newly derived exact formula;
- the original Morison equation approximation; and
- the original Morison's equation approximation with addition of fluid convective acceleration component.

It should be stressed that the important slam and slap forces associated with the impact of the wave surface on the structure are not considered in this study, which only treats structural members when fully immersed.

Although the size of the region of high accelerations is found to be relatively small (of order 1.5 metres square), the calculated inertial loads in the region are as high as the drag loads on a typical 1m radius member, contrary to the commonly-held view that, on a typical jacket structure in extreme waves, the fluid loading is dominated by drag forces.

Comparison of the different approximations of the inertial component shows that:

- Morison's equation is a very poor approximation.
- The addition of the convective acceleration term improves predictions but, contrary to the commonly-held view, this is not, in general, conservative.
- The degree of unconservatism of Morison's equation with convective acceleration components added is dependent on the orientation of the member to the wave.

Graphs are presented to show the variation in calculated components of fluid loading for different member orientations and different calculation methods.

1. INTRODUCTION

This is the report on a small study into the wave loads on the cylindrical members of offshore structures exposed to breaking waves. The topic is highly relevant to the development of the gas fields in the shallower coastal waters of the U.K. (e.g. southern North Sea, Morecambe Bay), because large breaking waves can occur there.

At present the wave loads on structures in these conditions are calculated by modest extrapolation of the methods used for calculating wave loads in non-breaking waves (e.g. Bartrop et al., 1987, Fig. G.2.1, which is a proposed revision by Atkins of the Dept. of Energy Design Guidance Notes) aided where appropriate by data derived empirically from model tests (e.g. Ochi & Tsai 1984).

In addition, it is current practice (see Bartrop et al. 1987, Section 3.5) to allow separately for the local wave slap and slam forces and pressures experienced as the member passes through the water surface. Consideration of these latter forces is beyond the scope of this work.

There have recently been two parallel theoretical developments which might allow breaking-wave loads to be calculated more scientifically. The first is the development of reliable computer programs to predict the detailed fluid flow in a breaking wave, see New et al. (1985). The fluid velocities given there are indeed no more than modest extrapolations of the velocities in non-breaking waves: the striking finding is that by contrast the fluid accelerations are not modest extrapolations of the accelerations in non-breaking waves, but are an order of magnitude higher (e.g. 5g compared with 0.5g). These accelerations would enter current fluid loading calculations through the inertia term in Morison's equation: there is however a problem here because Morison's equation was originally designed for applications where the fluid acceleration had a negligible convective constituent – Morison et al. originally considering "for simplicity of treatment" only waves of small amplitude, in which the convective constituent is negligible because it is of second order in waveheight. The problem is that in breaking waves that convective acceleration constituent is very large.

The standard procedure for dealing with this convective constituent is simply to include it in the acceleration figure used in the Morison inertia term (from which it was originally omitted), which is claimed by Isaacson (1979, 1981) to give answers which are conservative, although approximate. This claim is based on comparisons with loads calculated by Isaacson's own approach (Isaacson 1979 fig. 4), which is itself still only approximate, with Isaacson emphasising that, for all cases except a horizontal cylinder parallel to the wave crests, "a formally rigorous result is not guaranteed". Hitherto the only precise calculation has been that due to Lighthill (1979) on a vertical cylinder in small waves in deep water, where he showed that the load is as predicted by the original Morison inertia term, minus the additional load which would be predicted by Isaacson's own approach above (see Rainey 1989 eqn. 7.6). The one available precise calculation therefore throws doubt on Isaacson's claim that the standard procedure is conservative.

This brings in the second recent theoretical development, which is the resolution of that historical uncertainty over the inertia term in Morison's equation, through the derivation of an equivalent general-purpose fluid loading formula derived rigorously from first principles (and incidentally now implemented in a computer program under Dept. of Energy contract E/5B/CON/8041/2227, for the study of semisubmersible capsizes), see Rainey 1989. That formula is for the general case of a floating structure moving in waves, which has hitherto been the most prominent practical problem of inertial wave loading.

The objective of this report is to apply this formula (and Morison's equation too, with and without the convective acceleration included) to the relatively simple case of wave loading on the fully-immersed members of a fixed structure, and calculate the loads in a representative breaking wave described by the above theoretical model.

Not considered in this report is the contribution the new formula can also make to the calculation of the slam loading caused by a breaking wave. Existing methods are restricted to the case of simultaneous wave impact over a finite length of cylinder – in a breaking wave there is no such occurrence (except for a cylinder parallel to the wave crest), because the water surface is curved. Clearly, however, there is a slam-like phenomena caused by rapid changes in the cylinder's wetted length; the associated loads can also be calculated by the general form of the new formula, which is not restricted to cylinders immersed along their whole length.

The items of work in this study, in the order they are described in this report, are as follows:

- select a representative breaking wave (Section 2.1);
- calculate wave kinematics within the breaking wave separating total acceleration into its local and convective components (Sections 2.2 and 2.3);
- investigate spatial extent of high acceleration region of a breaking wave (Section 2.4);
- derive a general expression for the exact inertial component of fluid loading on a member (Section 3.1) and the expression for two special cases namely a cylinder parallel and perpendicular to the wave crest (Sections 3.2 and 3.3); and
- calculate inertial and drag components of fluid loading in a breaking wave and compare results obtained by Morison-type approximations (Section 4).

The breaking wave flow results reported by New et al. (1985) and the mathematical formulae derived in Rainey (1989) are used and referenced throughout this report. It is recommended that this report be studied in conjunction with both these papers as they contain a detailed description of notation and important background information.

2. WATER VELOCITY AND ACCELERATION IN A BREAKING WAVE

2.1 Selection of appropriate wave, wave height and wave period

This report is based on the breaking waves described in New et al.(1985); the first task is to choose an appropriate wave out of the nine described there, and to choose appropriate dimensions for it. Of the three high-resolution computations in New et al.(1985) (waves 1, 3 & 9 in Section 5 there), wave 9 is excluded because it is a deep-water breaking wave, whereas the primary UK offshore interest is in shallow-water breaking waves (see Section 1 above). Wave 3 is classed in New et al.(1985) as an "intermediate" case between a plunging breaker and a spilling breaker; referring to Atkins' proposed revision to the Dept. Energy Guidance notes (Bartrop et al. 1987, Fig 2.4.6) this does not appear any more common than a full plunging breaker, which apparently occurs over at least as wide a range of water depths, seabed slopes, and deep-water wave steepnesses. Accordingly the full plunging breaker, wave 1, was selected as the basis for the analyses in this report.

Suitable scale factors for this wave may be obtained from the Norwegian Maritime Directorate guidelines for Mobile Offshore Drilling Units, which define the recommended survival wave for the Viking area as having a height of 19 m and a period in the range 8.5 – 12.5 seconds. The water depth there is 30m, which is very typical of the UK southern North Sea and Morecambe Bay developments; this height and period range was therefore chosen.

The units of the data in New et al.(1985) are stated to be g's for acceleration and wavelengths for length, implying that the unit of velocity is the $\sqrt{(\text{wavelength} \times g)}$, and the unit of time is $\sqrt{(\text{wavelength}/g)}$. From the stated wave height:wavelength ratio of 0.11 we deduce that the length unit, as defined by New et al., in the case of our 19m high wave is

$$19 / 0.11 = 172.73\text{m}$$

so that the velocity unit in our case is:

$$\sqrt{(172.73 \times 9.81)} = 41.164 \text{ m/s}$$

and the time unit in our case is:

$$\sqrt{(172.73 / 9.81)} = 4.196 \text{ secs}$$

Finally the period of our 172.73 m long wave would be:

$$\sqrt{(172.73 \times 2\pi / 9.81)} = 10.52 \text{ secs}$$

in deep water (on linear theory), and somewhat longer in shallow water. This is consistent with the 8.5 to 12.5 secs range specified above by NMD.

2.2 Selection of appropriate time and location within wave

New et al.(1985) give (plotted in Figures 8(a) and 9(a)) the velocities and accelerations of a series of particles on the water surface, at a sequence of five points in time during the process of wave breaking. All this data was read off the figures manually, scaled to suit the selected 19 m Viking area waveheight as described above, and tabulated in Tables 1 to 5 below, which cover the sequence of five points in time. In addition, New et al.(1985) plot the successive positions of the water surface at the same points in time, in Figure 7(a); this is also entered in Tables 1 to 5. By comparing successive positions (using a standard cubic spline curve-fitting computer routine) an alternative figure for the velocity of each particle may be obtained, which is entered in Tables 1 to 5 as "position-based velocity". In all cases, the Tables give "X" and "Z" components, which are, following the

notation of Rainey (1989), the components in the horizontal direction of wave travel, and the upwards vertical direction.

An indication of the completeness of this data set for our purposes comes from the columns of the Tables which show the acceleration figures obtained by comparing (using the same curve-fitting computer routine) the velocities of a given particle at the five successive points in time; these are entitled "velocity-based acceleration" and "position-based acceleration" according to which of the two velocity figures above is used. These two figures should agree with each other and with the figures in the remaining acceleration columns in the Tables, which are obtained directly from the accelerations plotted in New et al.(1985). As can be seen, however, the agreement is only fair, there being differences of more than 50% for a good portion of the data. A close examination of the discrepancies shows that they are all associated either with a difficulty in reading accelerations accurately off the figures in New et al.(1985) (e.g. particle no. 40, 2nd point in time), or in reading velocities, or in reading positions. When two of these can be read accurately simultaneously (e.g. particle no. 40, 3rd point in time), the agreement is good; it is just that this happens surprisingly infrequently. The conclusion is that the quality of the computational procedure in New et al.(1985) is not in question, but that the results are unfortunately not presented in the full numerical detail which would be useful for our application (understandably, in view of the requirement for an attractive and readable paper).

For this reason initial attempts at using all the data in Tables 1 to 5 for a comprehensive series of computer calculations were abandoned, and it was decided instead to concentrate just on the important high-acceleration area of the wave (which after all was the motivation for this study, see Section 1 above). The time and location of highest acceleration was selected from Tables 1 to 5 – it is particle number 36, 5th point in time, whose acceleration is evidently 54.4 m/s/s horizontally, and 36.0 m/s/s vertically (downward). Referring to New et al.(1985), we see that this is the point right on the vertical face of the wave at its last stage of breaking, as shown in the last of the five profiles in Figure 7 (a) there.

In Section 2.3 below the required constituents of the acceleration at this point are derived from the data in Tables 1 to 5. In addition, Prof. Peregrine has kindly provided additional fine-mesh plots of velocities to complement Table 5, these are used in Section 2.4 below to illustrate the spatial extent of the high-acceleration region.

Table 1: Wave particle position, velocity and acceleration (horizontal and vertical)
time = 4.825 secs

Posn. no.	X position (m)		X velocity (m/s)		X acceleration (m/s/s)			Z position (m)		Z velocity (m/s)		Z acceleration (m/s/s)			
	New et al.	Posn. based	New et al.	Posn. based	New et al.	Vel. based	Posn. based	New et al.	Posn. based	New et al.	Vel. based	Posn. based	New et al.	Vel. based	Posn. based
31	120.405	-4.902	-5.140	0.316	-1.116	0.298	-4.208	-0.146	0.087	0.000	0.016	-0.059			
32	118.802	-4.986	-5.228	0.316	-1.476	0.598	-4.219	-0.116	0.162	0.000	-0.067	0.059			
33	117.220	-5.076	-5.291	0.316	-1.950	0.898	-4.219	-0.096	0.224	0.000	-0.194	0.357			
34	115.659	-5.161	-5.329	0.316	-2.455	1.197	-4.208	-0.070	0.274	0.000	-0.313	0.833			
35	114.119	-5.231	-5.341	0.316	-2.906	1.497	-4.187	-0.025	0.312	0.000	-0.371	1.487			
36	112.595	-5.278	-5.283	0.316	-3.220	1.580	-4.160	0.054	0.282	0.000	-0.314	2.438			
37	111.089	-5.291	-5.155	0.316	-3.313	1.449	-4.127	0.181	0.185	0.000	-0.088	3.687			
38	109.606	-5.260	-5.024	0.317	-3.101	1.425	-4.081	0.371	0.102	0.001	0.360	5.054			
39	108.153	-5.177	-4.959	0.317	-2.502	1.832	-4.016	0.638	0.117	0.001	1.084	6.362			
40	106.735	-5.031	-5.027	0.317	-1.431	2.995	-3.926	0.996	0.312	0.001	2.135	7.433			
41	105.349	-4.876	-5.349	0.317	0.333	5.151	-3.819	1.482	0.656	0.001	3.866	8.503			
42	103.990	-4.751	-5.879	0.318	2.826	8.087	-3.699	2.100	1.095	0.001	6.413	9.692			
43	102.665	-4.626	-6.437	0.318	5.854	11.442	-3.555	2.820	1.674	0.001	9.515	10.644			
44	101.381	-4.471	-6.842	0.318	9.223	14.857	-3.373	3.608	2.437	0.001	12.908	11.001			
45	100.142	-4.256	-6.912	0.318	12.740	17.973	-3.140	4.432	3.430	0.001	16.330	10.407			
46	98.933	-3.950	-6.724	0.318	16.209	21.196	-2.866	5.260	4.812	0.001	19.519	8.575			
47	97.750	-3.525	-6.397	0.319	19.439	24.767	-2.558	6.060	6.553	2.842	22.211	5.746			
48	96.617	-2.950	-5.819	4.116	22.234	28.075	-2.204	6.800	8.414	7.578	24.144	2.345			
49	95.560	-2.194	-4.877	8.863	24.402	30.508	-1.792	7.446	10.155	12.313	25.055	-1.199			
50	94.604	-1.229	-3.457	14.085	25.748	31.455	-1.308	7.968	11.537	14.680	24.681	-4.457			
51	93.733	0.047	-1.328	18.831	26.283	30.485	-0.733	8.404	12.624	14.679	22.707	-7.739			
52	92.929	1.658	1.435	23.102	26.215	28.005	-0.073	8.812	13.577	13.732	19.229	-11.330			
53	92.219	3.519	4.483	27.848	25.644	24.662	0.639	9.182	14.298	11.837	14.604	-14.767			
54	91.626	5.549	7.472	31.645	24.670	21.104	1.372	9.505	14.690	8.522	9.188	-17.585			
55	91.176	7.663	10.053	33.543	23.394	17.977	2.094	9.772	14.655	4.734	3.338	-19.321			
56	90.896	9.778	12.293	34.966	21.915	15.066	2.835	9.975	14.019	0.945	-2.589	-19.666			
57	90.767	11.811	14.422	35.441	20.333	11.939	3.616	10.104	12.847	-6.631	-8.236	-18.929			
58	90.753	13.678	16.342	33.067	18.749	8.919	4.393	10.150	11.400	-11.840	-13.247	-17.574			
59	90.814	15.296	17.956	29.270	17.262	6.331	5.121	10.105	9.941	-15.629	-17.265	-16.064			
60	90.913	16.580	19.165	24.524	15.974	4.498	5.758	9.959	8.731	-17.996	-19.934	-14.863			
61	91.080	17.561	19.819	20.251	14.727	3.707	6.290	9.665	7.755	-18.943	-21.309	-13.900			
62	91.339	18.341	19.982	16.454	13.330	3.744	6.746	9.206	6.840	-18.469	-21.791	-12.866			
63	91.647	18.947	19.881	13.132	11.833	4.175	7.146	8.620	6.007	-17.995	-21.541	-11.867			
64	91.959	19.406	19.743	10.759	10.284	4.570	7.508	7.941	5.278	-17.048	-20.720	-11.011			
65	92.231	19.744	19.793	8.860	8.732	4.498	7.851	7.207	4.677	-16.101	-19.489	-10.405			
66	92.472	19.990	20.087	7.728	7.225	3.791	8.167	6.455	4.243	-15.193	-18.009	-10.143			
67	92.710	20.169	20.475	6.605	5.812	2.737	8.444	5.719	3.961	-14.248	-16.441	-10.155			
68	92.934	20.310	20.872	5.572	4.541	1.587	8.693	5.038	3.772	-13.331	-14.945	-10.298			
69	93.130	20.438	21.196	4.714	3.462	0.592	8.927	4.447	3.615	-12.507	-13.682	-10.429			
70	93.286	20.582	21.364	4.114	2.623	0.005	9.160	3.983	3.430	-11.839	-12.815	-10.405			
71	93.402	20.701	21.312	3.717	2.042	-0.007	9.390	3.628	3.208	-11.293	-12.209	-10.179			
72	93.487	20.745	21.093	3.402	1.682	0.388	9.610	3.335	2.989	-10.789	-11.626	-9.846			
73	93.539	20.726	20.806	3.157	1.502	0.940	9.819	3.094	2.786	-10.321	-11.064	-9.477			
74	93.561	20.656	20.550	2.967	1.461	1.395	10.018	2.898	2.617	-9.884	-10.521	-9.145			
75	93.550	20.545	20.422	2.818	1.520	1.503	10.207	2.739	2.495	-9.471	-9.997	-8.919			
76	93.504	20.404	20.467	2.697	1.638	1.143	10.385	2.607	2.440	-9.077	-9.488	-8.847			
77	93.421	20.247	20.620	2.590	1.776	0.484	10.552	2.494	2.442	-8.696	-8.996	-8.883			
78	93.310	20.083	20.814	2.483	1.894	-0.295	10.709	2.393	2.472	-8.323	-8.516	-8.954			
79	93.175	19.924	20.980	2.363	1.951	-1.014	10.856	2.295	2.500	-7.952	-8.050	-8.990			
80	93.023	19.782	21.050	2.215	1.907	-1.493	10.992	2.191	2.495	-7.577	-7.594	-8.919			
81	92.850	19.645	21.035	2.051	1.796	-1.773	11.113	2.095	2.452	-7.203	-7.146	-8.716			
82	92.651	19.495	20.980	1.892	1.678	-1.852	11.220	2.025	2.392	-6.838	-6.705	-8.431			
83	92.434	19.334	20.869	1.738	1.553	-1.852	11.318	1.975	2.322	-6.483	-6.275	-8.098			
84	92.204	19.162	20.688	1.588	1.421	-1.733	11.415	1.941	2.250	-6.137	-5.859	-7.753			
85	91.968	18.981	20.422	1.444	1.281	-1.493	11.515	1.917	2.183	-5.801	-5.458	-7.432			
86	91.729	18.792	20.015	1.304	1.135	-1.014	11.628	1.899	2.125	-5.474	-5.076	-7.159			
87	91.485	18.597	19.477	1.168	0.981	-0.295	11.750	1.883	2.073	-5.157	-4.717	-6.909			
88	91.227	18.395	18.891	1.038	0.820	0.484	11.867	1.863	2.018	-4.849	-4.382	-6.647			
89	90.951	18.190	18.341	0.912	0.652	1.143	11.967	1.834	1.953	-4.551	-4.074	-6.338			
90	90.649	17.981	17.908	0.000	0.477	1.502	12.039	1.793	1.871	0.000	-3.797	-5.946			

Notes: New et al. - scaled from New et al. (1985)
Posn based - obtained by differentiating position data
Vel based - obtained by differentiating velocity data

Table 2: Wave particle position, velocity and acceleration (horizontal and vertical)
time = 5.245 secs

Posn. no.	X Position (m)		X velocity (m/s)		X acceleration (m/s/s)			Z position (m)		Z velocity (m/s)		Z acceleration (m/s/s)		
	New et al.	Posn. based	New et al.	Posn. based	New et al.	Vel. based	Posn. based	New et al.	New et al.	Posn. based	New et al.	Vel. based	Posn. based	
31	118.275	-5.083	-5.015	0.316	0.253	-0.230	-4.177	0.173	0.062	0.000	1.502	-5.414		
32	116.661	-5.194	-4.977	0.316	0.484	0.670	-4.145	0.357	0.187	0.000	2.322	-6.052		
33	115.079	-5.333	-4.914	0.316	0.725	0.979	-4.093	0.561	0.374	0.000	3.324	-6.329		
34	113.528	-5.465	-4.826	0.316	1.005	0.695	-4.020	0.792	0.624	0.000	4.422	-6.244		
35	112.009	-5.556	-4.713	0.316	1.356	-0.180	-3.926	1.058	0.935	0.000	5.533	-5.797		
36	110.517	-5.574	-4.620	0.316	1.808	-2.368	-3.827	1.367	1.305	0.000	6.572	-5.175		
37	109.053	-5.484	-4.547	0.317	2.392	-5.867	-3.725	1.727	1.731	2.842	7.453	-4.375		
38	107.623	-5.252	-4.427	5.063	3.139	-9.599	-3.593	2.145	2.223	7.577	8.092	-3.122		
39	106.233	-4.846	-4.190	9.810	4.080	-12.482	-3.406	2.629	2.787	12.313	8.405	-1.138		
40	104.889	-4.231	-3.771	13.608	5.245	-13.436	-3.140	3.187	3.430	14.681	8.307	1.856		
41	103.558	-3.367	-3.188	15.981	6.859	-12.478	-2.795	3.920	4.224	13.734	7.756	6.882		
42	102.235	-2.266	-2.486	18.355	9.014	-10.328	-2.387	4.876	5.162	12.313	6.816	13.775		
43	100.971	-0.975	-1.636	20.728	11.545	-6.962	-1.916	5.983	6.140	10.419	5.563	20.941		
44	99.817	0.461	-0.608	23.101	14.283	-2.351	-1.382	7.171	7.053	8.998	4.072	26.905		
45	98.824	1.998	0.628	25.475	17.063	3.531	-0.785	8.366	7.796	7.577	2.417	30.113		
46	97.978	3.588	2.169	27.848	19.717	12.217	-0.092	9.497	8.410	5.209	0.673	30.229		
47	97.246	5.187	3.995	30.221	22.080	23.692	0.697	10.493	8.964	2.841	-1.085	28.275		
48	96.647	6.748	5.960	32.595	23.985	35.651	1.533	11.282	9.398	0.473	-2.783	24.757		
49	96.199	8.227	7.924	34.968	25.264	45.793	2.364	11.791	9.652	-1.895	-4.345	20.179		
50	95.923	9.577	9.741	37.816	25.751	51.816	3.141	11.951	9.667	-3.789	-5.697	15.044		
51	95.860	10.878	11.463	37.816	25.336	52.830	3.884	11.709	9.378	-12.314	-6.956	8.304		
52	95.997	12.221	13.185	34.018	24.131	50.371	4.627	11.113	8.824	-18.944	-8.264	-0.376		
53	96.271	13.579	14.831	26.898	22.302	45.771	5.339	10.235	8.103	-23.206	-9.585	-9.424		
54	96.619	14.925	16.327	19.778	20.015	40.363	5.988	9.149	7.312	-24.627	-10.882	-17.269		
55	96.978	16.230	17.596	14.082	17.435	35.478	6.543	7.930	6.548	-23.680	-12.120	-22.337		
56	97.381	17.467	18.614	9.810	14.729	30.541	6.987	6.649	5.767	-21.785	-13.261	-23.985		
57	97.870	18.608	19.431	6.962	12.063	24.662	7.340	5.382	4.904	-19.891	-14.270	-23.263		
58	98.396	19.626	20.085	5.063	9.602	18.708	7.629	4.200	4.026	-17.996	-15.110	-21.133		
59	98.906	20.494	20.613	4.114	7.512	13.543	7.878	3.178	3.200	-16.575	-15.745	-18.561		
60	99.351	21.182	21.052	3.164	5.960	10.034	8.113	2.390	2.494	-15.155	-16.138	-16.511		
61	99.723	21.670	21.374	0.316	4.855	8.851	8.320	1.787	1.923	-13.734	-16.238	-14.743		
62	100.054	21.972	21.553	0.316	3.973	9.419	8.484	1.267	1.442	-11.366	-16.051	-12.617		
63	100.358	22.119	21.633	0.316	3.283	10.728	8.622	0.820	1.028	-6.630	-15.633	-10.487		
64	100.647	22.141	21.661	0.316	2.754	11.774	8.754	0.438	0.659	-1.894	-15.041	-8.714		
65	100.934	22.070	21.681	0.316	2.354	11.547	8.898	0.112	0.312	0.000	-14.329	-6.753		
66	101.235	21.936	21.678	0.316	2.052	9.521	9.055	-0.167	-0.013	0.202	-13.552	-7.613		
67	101.543	21.770	21.623	0.316	1.816	6.367	9.212	-0.409	-0.299	0.227	-12.768	-8.357		
68	101.832	21.602	21.537	0.316	1.615	2.877	9.369	-0.622	-0.549	0.152	-12.030	-9.421		
69	102.077	21.462	21.444	0.316	1.418	-0.158	9.526	-0.814	-0.761	0.051	-11.394	-10.342		
70	102.252	21.382	21.367	0.316	1.192	-1.947	9.683	-0.996	-0.936	0.000	-10.917	-10.655		
71	102.345	21.336	21.309	0.316	0.986	-2.010	9.840	-1.150	-1.063	0.000	-10.567	-10.148		
72	102.372	21.278	21.256	0.316	0.858	-0.870	9.997	-1.259	-1.143	0.000	-10.268	-9.130		
73	102.353	21.208	21.201	0.316	0.795	0.742	10.154	-1.328	-1.190	0.000	-10.011	-7.920		
74	102.307	21.126	21.135	0.316	0.782	2.116	10.311	-1.362	-1.220	0.000	-9.786	-6.841		
75	102.252	21.032	21.052	0.316	0.805	2.531	10.468	-1.369	-1.247	0.000	-9.582	-6.211		
76	102.193	20.926	20.947	0.316	0.849	1.673	10.630	-1.355	-1.272	0.000	-9.391	-6.175		
77	102.117	20.808	20.824	0.316	0.900	0.022	10.795	-1.324	-1.285	0.000	-9.201	-6.518		
78	102.018	20.678	20.690	0.316	0.944	-1.953	10.958	-1.283	-1.285	0.000	-9.003	-7.026		
79	101.889	20.536	20.555	0.316	0.967	-3.784	11.113	-1.238	-1.272	0.000	-8.788	-7.486		
80	101.725	20.382	20.424	0.316	0.954	-5.003	11.253	-1.195	-1.247	0.000	-8.544	-7.683		
81	101.524	20.215	20.308	0.316	0.921	-5.632	11.375	-1.141	-1.205	0.000	-8.280	-7.969		
82	101.292	20.035	20.203	0.316	0.893	-5.985	11.482	-1.063	-1.145	0.000	-8.012	-8.487		
83	101.029	19.841	20.092	0.316	0.866	-6.025	11.580	-0.965	-1.075	0.000	-7.739	-8.710		
84	100.733	19.636	19.961	0.316	0.837	-5.719	11.676	-0.854	-1.003	0.000	-7.462	-8.107		
85	100.406	19.419	19.795	0.316	0.805	-5.032	11.777	-0.735	-0.936	0.000	-7.179	-6.152		
86	100.039	19.191	19.589	0.316	0.765	-3.604	11.890	-0.612	-0.878	0.000	-6.892	-2.115		
87	99.632	18.952	19.353	0.316	0.715	-1.459	12.011	-0.492	-0.826	0.000	-6.600	3.652		
88	99.197	18.704	19.094	0.316	0.652	0.865	12.129	-0.379	-0.771	0.000	-6.304	10.055		
89	98.748	18.447	18.820	0.316	0.574	2.829	12.229	-0.280	-0.706	0.000	-6.002	16.000		
90	98.297	18.181	18.539	0.000	0.477	3.894	12.300	-0.199	-0.623	0.000	-5.696	20.395		

Notes: New et al. - scaled from New et al. (1985)
Posn based - obtained by differentiating position data
Vel based - obtained by differentiating velocity data

Table 3: Wave particle position, velocity and acceleration (horizontal and vertical)
time = 5.665 secs

Posn. no.	X Position (m)			X velocity (m/s)			X acceleration (m/s/s)			Z position (m)			Z velocity (m/s)			Z acceleration (m/s/s)		
	New et al.	New et al.	Posn. based	New et al.	Vel. based	Posn. based	New et al.	Vel. based	Posn. based	New et al.	New et al.	Posn. based	New et al.	New et al.	Posn. based	New et al.	Vel. based	Posn. based
31	116.197	-4.689	-4.779	0.316	2.134	1.355	-4.156	1.115	1.161	0.000	3.227	10.651						
32	114.625	-4.580	-4.741	0.316	3.758	0.453	-4.062	1.832	1.494	0.000	4.183	12.284						
33	113.096	-4.468	-4.555	0.316	5.702	0.735	-3.905	2.693	1.927	0.000	5.336	13.729						
34	111.608	-4.317	-4.219	0.316	7.847	2.201	-3.685	3.641	2.458	0.000	6.570	14.986						
35	110.163	-4.093	-3.733	0.316	10.078	4.850	-3.402	4.619	3.088	0.000	7.769	16.056						
36	108.718	-3.760	-3.129	0.316	12.276	9.477	-3.065	5.569	3.925	0.000	8.817	17.664						
37	107.273	-3.283	-2.404	5.063	14.326	10.082	-2.674	6.436	4.970	2.842	9.596	19.812						
38	105.891	-2.625	-1.516	9.810	16.110	23.477	-2.215	7.163	6.059	4.736	9.992	21.408						
39	104.636	-1.752	-0.418	13.607	17.512	30.463	-1.677	7.692	7.030	9.472	9.887	21.363						
40	103.570	-0.629	0.933	18.354	18.414	35.857	-1.047	7.967	7.719	12.313	9.165	18.586						
41	102.674	0.881	2.673	23.101	18.847	40.412	-0.274	7.990	8.132	7.577	7.611	11.784						
42	101.904	2.814	4.771	27.848	18.947	44.921	0.632	7.821	8.376	2.842	5.226	1.567						
43	101.292	5.063	7.026	32.595	18.760	48.253	1.597	7.489	8.445	-1.894	2.219	-9.951						
44	100.870	7.516	9.236	37.341	18.331	49.276	2.546	7.026	8.332	-6.630	-1.203	-20.809						
45	100.670	10.064	11.200	41.139	17.706	46.860	3.402	6.461	8.028	-10.419	-4.832	-29.008						
46	100.754	12.597	12.948	38.291	16.930	39.156	4.192	5.826	7.465	-20.838	-8.460	-34.734						
47	101.102	15.005	14.613	29.746	16.048	26.919	4.964	5.150	6.647	-27.942	-11.878	-39.317						
48	101.619	17.179	16.151	19.778	15.105	12.921	5.682	4.465	5.679	-28.889	-14.880	-42.483						
49	102.210	19.007	17.517	12.183	14.148	-0.066	6.308	3.800	4.664	-26.521	-17.256	-43.956						
50	102.779	20.382	18.667	7.437	13.220	-9.270	6.804	3.187	3.705	-23.679	-18.799	-43.461						
51	103.353	21.310	19.566	4.114	12.194	-14.209	7.137	2.567	2.764	-20.838	-19.506	-39.827						
52	103.994	21.909	20.243	2.690	10.950	-16.730	7.332	1.877	1.771	-18.470	-19.591	-33.240						
53	104.665	22.236	20.750	1.740	9.550	-17.558	7.439	1.139	0.785	-16.102	-19.171	-25.452						
54	105.328	22.346	21.141	1.266	8.053	-7.416	7.508	0.373	-0.133	-14.681	-18.363	-18.218						
55	105.944	22.295	21.467	0.791	6.522	-17.028	7.590	-0.398	-0.926	-13.734	-17.287	-13.291						
56	106.518	22.140	21.689	0.316	5.016	-15.887	7.675	-1.154	-1.578	-12.313	-16.058	-11.028						
57	107.075	21.935	21.771	0.316	3.598	-13.511	7.732	-1.872	-2.129	-11.366	-14.796	-10.262						
58	107.608	21.736	21.773	0.316	2.327	-10.659	7.772	-2.530	-2.601	-10.892	-13.618	-10.455						
59	108.113	21.600	21.756	0.316	1.265	-8.094	7.807	-3.109	-3.016	-10.419	-12.642	-11.069						
60	108.581	21.583	21.778	0.316	0.472	-6.574	7.851	-3.585	-3.396	-9.945	-11.985	-11.568						
61	109.018	21.636	21.850	0.316	-0.044	-6.581	7.904	-3.962	-3.732	-9.472	-11.561	-12.214						
62	109.427	21.675	21.933	0.316	-0.344	-7.608	7.956	-4.264	-4.009	-8.998	-11.203	-13.364						
63	109.802	21.702	22.010	0.316	-0.465	-8.933	8.008	-4.500	-4.241	-8.525	-10.900	-14.626						
64	110.138	21.717	22.067	0.316	-0.446	-9.837	8.061	-4.682	-4.444	-8.051	-10.644	-15.606						
65	110.427	21.720	22.089	0.316	-0.325	-9.600	8.113	-4.818	-4.631	-7.577	-10.428	-15.909						
66	110.665	21.712	22.067	0.316	-0.140	-7.668	8.157	-4.919	-4.799	-7.437	-10.242	-15.203						
67	110.857	21.694	22.010	0.316	0.071	-4.524	8.193	-4.996	-4.938	-7.327	-10.078	-13.751						
68	111.009	21.666	21.933	0.316	0.268	-0.993	8.232	-5.058	-5.054	-7.240	-9.928	-12.015						
69	111.127	21.628	21.850	0.316	0.415	2.094	8.289	-5.115	-5.155	-7.168	-9.783	-10.603						
70	111.218	21.583	21.778	0.316	0.472	3.910	8.375	-5.179	-5.249	-7.104	-9.635	-9.904						
71	111.285	21.528	21.726	0.316	0.471	3.999	8.498	-5.239	-5.340	-7.071	-9.503	-10.240						
72	111.326	21.466	21.684	0.316	0.468	2.912	8.651	-5.282	-5.424	-7.087	-9.407	-11.279						
73	111.332	21.394	21.636	0.316	0.465	1.335	8.821	-5.307	-5.493	-7.132	-9.339	-12.592						
74	111.298	21.312	21.569	0.316	0.461	-0.048	8.994	-5.314	-5.540	-7.187	-9.291	-13.753						
75	111.218	21.220	21.467	0.316	0.457	-0.554	9.160	-5.303	-5.558	-7.232	-9.253	-14.334						
76	111.083	21.117	21.315	0.316	0.455	0.084	9.317	-5.274	-5.545	-7.248	-9.217	-14.192						
77	110.897	21.002	21.124	0.316	0.455	1.408	9.474	-5.227	-5.508	-7.215	-9.176	-13.613						
78	110.674	20.875	20.915	0.316	0.457	3.022	9.631	-5.163	-5.447	-7.114	-9.120	-12.810						
79	110.425	20.735	20.711	0.316	0.463	4.527	9.788	-5.080	-5.360	-6.925	-9.040	-11.998						
80	110.163	20.582	20.534	0.316	0.472	5.527	9.945	-4.980	-5.249	-6.630	-8.930	-11.390						
81	109.893	20.418	20.399	0.316	0.494	6.067	10.102	-4.854	-5.019	-6.244	-8.802	-10.211						
82	109.606	20.244	20.292	0.316	0.531	6.412	10.259	-4.699	-4.671	-5.797	-8.674	-8.318						
83	109.296	20.060	20.190	0.316	0.578	6.494	10.416	-4.520	-4.345	-5.288	-8.541	-6.875						
84	108.956	19.865	20.071	0.316	0.629	6.242	10.573	-4.321	-4.182	-4.717	-8.398	-7.045						
85	108.581	19.657	19.912	0.316	0.679	5.586	10.730	-4.108	-4.323	-4.085	-8.239	-9.992						
86	108.169	19.434	19.707	0.316	0.721	4.167	10.891	-3.885	-4.940	-3.391	-8.061	-17.247						
87	107.726	19.197	19.474	0.316	0.751	2.033	11.057	-3.656	-5.941	-2.636	-7.858	-20.032						
88	107.252	18.943	19.217	0.316	0.763	-0.279	11.220	-3.428	-7.064	-1.819	-7.625	-40.053						
89	106.745	18.671	18.946	0.316	0.750	-2.230	11.375	-3.203	-8.052	-0.940	-7.357	-51.018						
90	106.208	18.381	18.667	0.000	0.708	-3.282	11.515	-2.988	-8.645	0.000	-7.050	-58.631						

Notes: New et al. - scaled from New et al. (1985)
Posn based - obtained by differentiating position data
Vel based - obtained by differentiating velocity data

Table 4: Wave particle position, velocity and acceleration (horizontal and vertical)
time = 6.093 secs

Posn. no.	X Position (m)		X velocity (m/s)			X acceleration (m/s/s)			Z position (m)		Z velocity (m/s)			Z acceleration (m/s/s)		
	New et al.	Posn. based	New et al.	Posn. based	Vel. based	New et al.	Posn. based	Vel. based	New et al.	Posn. based	New et al.	Posn. based	Vel. based	New et al.	Posn. based	Vel. based
31	114.224	-3.274	-3.634	4.417	5.007	8.318	-3.193	2.908	3.878	8.449	5.185	10.212				
32	112.642	-2.009	-3.211	5.974	7.360	12.791	-2.879	3.902	5.076	11.139	3.737	15.675				
33	111.218	-0.500	-2.464	8.329	10.164	17.187	-2.460	5.084	6.064	11.972	1.887	18.356				
34	109.952	1.186	-1.394	11.025	13.222	21.503	-1.937	6.361	6.842	12.010	-0.246	18.166				
35	108.845	2.985	0.000	13.607	16.333	25.741	-1.309	7.644	7.410	12.313	-2.540	15.103				
36	107.866	4.831	1.916	18.354	19.299	31.206	-0.500	8.840	7.773	7.578	-4.875	6.980				
37	107.015	6.659	4.355	23.101	21.922	37.899	0.488	9.861	7.931	2.842	-7.131	-6.203				
38	106.338	8.403	7.018	27.848	24.000	43.860	1.543	10.614	7.877	-1.894	-9.187	-21.165				
39	105.878	9.997	9.606	37.341	25.337	47.129	2.552	11.009	7.603	-6.630	-10.923	-34.620				
40	105.680	11.377	11.821	46.360	25.732	45.746	3.402	10.955	7.102	-13.734	-12.217	-43.286				
41	105.823	12.607	13.683	43.512	25.026	37.209	4.097	10.371	6.274	-30.783	-13.130	-46.554				
42	106.279	13.793	15.391	28.797	23.335	22.824	4.713	9.306	5.126	-38.360	-13.819	-46.613				
43	106.927	14.925	16.914	15.507	20.878	6.345	5.242	7.864	3.804	-35.045	-14.312	-44.376				
44	107.646	15.999	18.223	6.962	17.872	-8.475	5.680	6.151	2.458	-29.362	-14.635	-40.756				
45	108.317	17.005	19.289	3.165	14.533	-17.881	6.019	4.270	1.235	-23.679	-14.818	-36.664				
46	108.952	17.937	20.050	1.741	11.080	-20.633	6.235	2.327	0.102	-20.838	-14.886	-31.102				
47	109.631	18.788	20.528	0.317	7.730	-19.235	6.331	0.425	-1.042	-18.470	-14.868	-23.460				
48	110.336	19.551	20.812	0.317	4.700	-15.546	6.346	-1.330	-2.144	-16.102	-14.790	-15.239				
49	111.047	20.218	20.991	0.317	2.208	-11.425	6.317	-2.835	-3.152	-13.734	-14.682	-7.938				
50	111.745	20.782	21.155	0.317	0.472	-8.732	6.281	-3.983	-4.014	-11.366	-14.569	-3.054				
51	112.443	21.213	21.270	0.316	-0.583	-7.541	6.227	-4.824	-4.695	-6.630	-14.379	-1.137				
52	113.154	21.502	21.275	0.316	-1.221	-6.611	6.128	-5.492	-5.231	-1.895	-14.044	-1.185				
53	113.859	21.674	21.222	0.316	-1.514	-5.832	6.005	-6.014	-5.673	0.000	-13.597	-2.379				
54	114.538	21.751	21.165	0.316	-1.536	-5.094	5.875	-6.415	-6.074	0.000	-13.071	-3.898				
55	115.173	21.758	21.155	0.316	-1.358	-4.285	5.758	-6.722	-6.484	0.000	-12.498	-4.920				
56	115.764	21.719	21.197	0.316	-1.052	-3.408	5.649	-6.962	-6.908	0.000	-11.913	-5.560				
57	116.323	21.658	21.257	0.316	-0.691	-2.535	5.536	-7.160	-7.314	0.000	-11.347	-6.365				
58	116.850	21.599	21.327	0.316	-0.348	-1.665	5.425	-7.342	-7.691	0.000	-10.835	-7.164				
59	117.346	21.566	21.399	0.316	-0.093	-0.795	5.322	-7.536	-8.035	0.000	-10.410	-7.786				
60	117.810	21.583	21.466	0.316	0.000	0.075	5.234	-7.768	-8.336	0.000	-10.104	-8.059				
61	118.243	21.632	21.533	0.316	-0.004	1.179	5.157	-8.012	-8.595	0.000	-9.911	-7.801				
62	118.644	21.680	21.605	0.316	0.006	2.514	5.086	-8.228	-8.818	0.000	-9.794	-7.126				
63	119.013	21.724	21.675	0.316	0.026	3.733	5.027	-8.418	-9.003	0.000	-9.737	-6.307				
64	119.350	21.763	21.735	0.316	0.055	4.489	4.987	-8.584	-9.151	0.000	-9.728	-5.621				
65	119.656	21.795	21.777	0.316	0.089	4.437	4.973	-8.727	-9.262	0.000	-9.752	-5.343				
66	119.939	21.818	21.802	0.316	0.125	3.114	4.987	-8.848	-9.317	0.000	-9.794	-5.675				
67	120.198	21.830	21.815	0.316	0.160	0.751	5.027	-8.951	-9.314	0.000	-9.841	-6.436				
68	120.422	21.829	21.815	0.316	0.193	-1.959	5.086	-9.036	-9.285	0.000	-9.878	-7.319				
69	120.597	21.814	21.802	0.316	0.219	-4.324	5.157	-9.106	-9.257	0.000	-9.893	-8.018				
70	120.711	21.783	21.777	0.316	0.236	-5.654	5.234	-9.162	-9.262	0.000	-9.869	-8.228				
71	120.760	21.736	21.735	0.316	0.244	-5.672	5.314	-9.205	-9.319	0.000	-9.820	-7.746				
72	120.751	21.675	21.675	0.316	0.244	-4.839	5.400	-9.232	-9.408	0.000	-9.766	-6.775				
73	120.692	21.602	21.606	0.316	0.239	-3.569	5.498	-9.243	-9.499	0.000	-9.707	-5.621				
74	120.589	21.517	21.533	0.316	0.230	-2.277	5.615	-9.237	-9.564	0.000	-9.644	-4.589				
75	120.447	21.420	21.466	0.316	0.221	-1.378	5.758	-9.212	-9.571	0.000	-9.575	-3.985				
76	120.260	21.312	21.419	0.316	0.213	-0.802	5.929	-9.167	-9.512	0.000	-9.503	-3.853				
77	120.021	21.194	21.386	0.316	0.209	-0.272	6.126	-9.101	-9.406	0.000	-9.425	-3.990				
78	119.745	21.065	21.347	0.316	0.210	0.106	6.342	-9.012	-9.267	0.000	-9.343	-4.329				
79	119.443	20.928	21.277	0.316	0.218	0.228	6.570	-8.900	-9.112	0.000	-9.256	-4.802				
80	119.129	20.782	21.155	0.316	0.236	-0.010	6.804	-8.764	-8.954	0.000	-9.164	-5.343				
81	118.815	20.633	20.961	0.316	0.268	-1.001	7.121	-8.602	-8.798	0.000	-9.086	-6.027				
82	118.492	20.484	20.710	0.316	0.315	-2.676	7.523	-8.415	-8.635	0.000	-9.031	-12.899				
83	118.142	20.331	20.431	0.316	0.373	-4.445	7.897	-8.205	-8.457	0.000	-8.987	-16.845				
84	117.745	20.169	20.155	0.316	0.436	-5.719	8.132	-7.972	-8.257	0.000	-8.942	-16.751				
85	117.283	19.994	19.911	0.316	0.502	-5.910	8.113	-7.718	-8.027	0.000	-8.885	-9.502				
86	116.743	19.802	19.714	0.316	0.565	-4.486	7.703	-7.444	-7.768	0.000	-8.803	8.757				
87	116.137	19.589	19.545	0.316	0.621	-1.841	6.976	-7.152	-7.484	0.000	-8.685	35.949				
88	115.486	19.351	19.380	0.316	0.667	1.231	6.141	-6.842	-7.176	0.000	-8.518	66.292				
89	114.806	19.083	19.199	0.316	0.697	3.931	5.404	-6.516	-6.843	0.000	-8.290	94.004				
90	114.118	18.781	18.977	0.000	0.708	5.464	4.973	-6.175	-6.485	0.000	-7.989	113.301				

Notes: New et al. - scaled from New et al. (1985)
Posn based - obtained by differentiating position data
Vel based - obtained by differentiating velocity data

Table 5: Wave particle position, velocity and acceleration (horizontal and vertical)
time = 6.512 secs

Posn. no.	X Position (m)			X velocity (m/s)			X acceleration (m/s/s)			Z position (m)			Z velocity (m/s)			Z acceleration (m/s/s)		
	New et al.	New et al.	Posn. based	New et al.	Vel. based	Posn. based	New et al.	Vel. based	Posn. based	New et al.	New et al.	Posn. based	New et al.	New et al.	Posn. based	New et al.	Vel. based	Posn. based
31	113.117	-0.445	-1.664	18.851	8.443	4.554	-0.869	5.510	7.165	20.216	7.196	7.603						
32	111.904	1.658	-0.337	27.155	10.092	6.646	0.241	5.000	9.745	19.163	1.517	10.799						
33	111.007	4.148	1.420	34.689	11.971	8.982	1.235	4.293	11.494	11.507	-5.583	12.558						
34	110.427	6.890	3.607	41.892	13.954	11.564	2.114	3.433	12.411	1.020	-13.580	12.879						
35	110.163	9.751	6.222	49.206	15.917	14.390	2.879	2.465	12.496	-8.523	-21.948	11.762						
36	110.342	12.598	9.809	54.428	17.734	18.253	3.523	1.436	11.369	-35.989	-30.164	8.317						
37	110.964	15.298	14.367	33.069	19.280	23.154	4.049	0.391	9.031	-50.196	-37.701	2.544						
38	111.840	17.718	19.084	12.660	20.431	27.903	4.461	-0.625	6.051	-41.673	-44.036	-4.222						
39	112.779	19.723	23.147	3.642	21.061	31.313	4.767	-1.567	3.000	-31.729	-48.643	-10.644						
40	113.591	21.182	25.744	-0.154	21.045	32.197	4.972	-2.389	0.448	-23.679	-50.998	-15.386						
41	114.272	22.093	26.458	0.320	20.229	29.542	5.044	-3.140	-1.685	-20.839	-50.890	-18.405						
42	114.949	22.594	25.829	0.319	18.658	24.140	4.977	-3.893	-3.780	-18.472	-48.744	-20.594						
43	115.629	22.760	24.485	0.317	16.503	17.509	4.822	-4.643	-5.715	-16.104	-44.993	-22.014						
44	116.316	22.664	23.052	0.316	13.936	11.168	4.629	-5.380	-7.369	-13.736	-40.071	-22.726						
45	117.019	22.383	22.157	0.316	11.131	6.635	4.449	-6.099	-8.621	-11.367	-34.409	-22.793						
46	117.749	21.989	21.859	0.316	8.258	4.183	4.278	-6.792	-9.337	-8.999	-28.441	-22.828						
47	118.502	21.558	21.739	0.316	5.490	2.800	4.081	-7.452	-9.600	-6.631	-22.599	-19.790						
48	119.259	21.163	21.709	0.316	2.999	2.076	3.865	-8.072	-9.606	-4.263	-17.315	-17.258						
49	120.002	20.880	21.683	0.316	0.957	1.601	3.637	-8.644	-9.557	-1.895	-13.024	-14.813						
50	120.711	20.782	21.572	0.316	-0.463	0.964	3.402	-9.162	-9.650	-0.001	-10.156	-13.036						
51	121.382	20.816	21.330	0.316	-1.303	0.140	3.157	-9.621	-9.881	0.000	-8.540	-11.993						
52	122.027	20.875	21.017	0.316	-1.765	-0.596	2.898	-10.027	-10.117	0.000	-7.632	-11.298						
53	122.654	20.953	20.700	0.316	-1.917	-1.209	2.630	-10.387	-10.365	0.000	-7.306	-10.849						
54	123.268	21.045	20.447	0.316	-1.826	-1.660	2.360	-10.706	-10.635	0.000	-7.436	-10.548						
55	123.875	21.145	20.327	0.316	-1.561	-1.914	2.094	-10.992	-10.934	0.000	-7.898	-10.292						
56	124.485	21.248	20.376	0.316	-1.190	-1.901	1.820	-11.251	-11.298	0.000	-8.564	-10.152						
57	125.093	21.349	20.546	0.316	-0.780	-1.645	1.533	-11.490	-11.721	0.000	-9.311	-10.193						
58	125.685	21.442	20.786	0.316	-0.400	-1.250	1.252	-11.715	-12.151	0.000	-10.011	-10.313						
59	126.251	21.521	21.044	0.316	-0.117	-0.821	0.997	-11.933	-12.536	0.000	-10.541	-10.409						
60	126.776	21.583	21.267	0.316	0.000	-0.461	0.785	-12.150	-12.823	0.000	-10.773	-10.377						
61	127.270	21.632	21.490	0.316	0.004	-0.101	0.618	-12.364	-12.994	0.000	-10.818	-10.171						
62	127.740	21.680	21.747	0.316	-0.006	0.328	0.482	-12.566	-13.082	0.000	-10.867	-9.862						
63	128.175	21.724	21.988	0.316	-0.026	0.723	0.377	-12.754	-13.118	0.000	-10.915	-9.516						
64	128.561	21.763	22.158	0.316	-0.054	0.979	0.304	-12.927	-13.131	0.000	-10.961	-9.203						
65	128.886	21.795	22.206	0.316	-0.087	0.992	0.262	-13.083	-13.150	0.000	-11.001	-8.991						
66	129.145	21.818	22.072	0.316	-0.122	0.625	0.260	-13.221	-13.176	0.000	-11.032	-8.925						
67	129.348	21.830	21.791	0.316	-0.157	-0.054	0.298	-13.337	-13.188	0.000	-11.051	-8.959						
68	129.500	21.829	21.453	0.316	-0.189	-0.836	0.362	-13.431	-13.188	0.000	-11.055	-9.026						
69	129.607	21.814	21.146	0.316	-0.215	-1.516	0.442	-13.501	-13.175	0.000	-11.040	-9.059						
70	129.677	21.783	20.962	0.316	-0.231	-1.886	0.524	-13.544	-13.150	0.000	-11.004	-8.991						
71	129.709	21.735	20.924	0.316	-0.243	-1.876	0.599	-13.563	-13.114	0.000	-10.940	-8.776						
72	129.698	21.672	20.972	0.316	-0.254	-1.626	0.677	-13.560	-13.066	0.000	-10.849	-8.460						
73	129.645	21.596	21.070	0.316	-0.264	-1.327	0.769	-13.535	-13.006	0.000	-10.737	-8.110						
74	129.550	21.507	21.181	0.316	-0.271	-0.815	0.888	-13.488	-12.934	0.000	-10.608	-7.793						
75	129.413	21.407	21.267	0.316	-0.276	-0.461	1.047	-13.420	-12.847	0.000	-10.469	-7.577						
76	129.238	21.298	21.373	0.316	-0.277	-0.106	1.254	-13.329	-12.737	0.000	-10.325	-7.460						
77	129.025	21.179	21.524	0.316	-0.274	0.318	1.501	-13.216	-12.604	0.000	-10.182	-7.398						
78	128.768	21.053	21.653	0.316	-0.266	0.708	1.776	-13.082	-12.463	0.000	-10.046	-7.391						
79	128.460	20.920	21.691	0.316	-0.252	0.958	2.065	-12.926	-12.329	0.000	-9.921	-7.441						
80	128.095	20.782	21.572	0.316	-0.231	0.964	2.356	-12.747	-12.218	0.000	-9.815	-7.549						
81	127.660	20.645	21.195	0.316	-0.207	0.541	2.645	-12.555	-12.499	0.000	-9.750	-8.558						
82	127.160	20.512	20.605	0.316	-0.181	-0.242	2.940	-12.354	-13.162	0.000	-9.735	-10.470						
83	126.614	20.376	19.952	0.316	-0.152	-1.107	3.248	-12.138	-13.653	0.000	-9.750	-12.016						
84	126.040	20.235	19.387	0.316	-0.118	-1.776	3.574	-11.901	-13.414	0.000	-9.777	-11.927						
85	125.458	20.082	19.058	0.316	-0.079	-1.971	3.926	-11.639	-11.891	0.000	-9.795	-8.934						
86	124.880	19.913	19.072	0.316	-0.032	-1.485	4.307	-11.347	-8.410	0.000	-9.785	-1.485						
87	124.293	19.723	19.327	0.316	0.022	-0.502	4.713	-11.018	-3.343	0.000	-9.729	9.576						
88	123.679	19.508	19.668	0.316	0.087	0.664	5.138	-10.647	2.302	0.000	-9.607	21.917						
89	123.019	19.262	19.935	0.316	0.162	1.704	5.575	-10.230	7.518	0.000	-9.399	33.209						
90	122.293	18.981	19.973	0.000	0.250	2.304	6.019	-9.760	11.297	0.000	-9.087	41.120						

Notes: New et al. - scaled from New et al. (1985)
Posn based - obtained by differentiating position data
Vel based - obtained by differentiating velocity data

2.3 Acceleration constituents at chosen point

The remaining task is to determine the fluid acceleration behaviour at our chosen point in full detail. As noted in Section 1, this means addressing the well-known problem that the acceleration of a fluid particle has two constituents which are:

- characteristic of a flow field which is changing as a whole from one instant to the next (as it patently is in our case); and
- characteristic of a flow field which may be the same at all times, but is spatially non-uniform (as ours patently is also; a simpler example would be steady flow through a narrowing pipe, where the fluid particles clearly must be accelerating).

Mathematically, the acceleration \underline{a} of a fluid particle whose velocity is \underline{v} can accordingly be written (see e.g. Batchelor, 1967, eqn. 2.1.2) as the sum of a local acceleration $\dot{\underline{v}}$ (written $\partial\underline{v}/\partial t$ by Batchelor), which describes the effect of changes in the flow-field with time, and a convective acceleration $V\underline{v}$, which describes the effects present even when the flow-field does not change with time:

$$\underline{a} = \dot{\underline{v}} + V\underline{v}$$

The matrix V (written $\nabla\underline{v}$ by Batchelor) defines the velocity gradient in the flow at the point in question. That is to say, if we move a small distance $\delta\underline{x}$ in the fluid, we will observe a change in velocity $\delta\underline{v}$ given by:

$$\delta\underline{v} = V\delta\underline{x}$$

We need to know this matrix as well as \underline{a} and \underline{v} to apply the fluid loading formula in Rainey (1989); we also need to know the local acceleration $\dot{\underline{v}}$ to calculate the original Morison inertia term, in which the convective acceleration is ignored.

In our case of long-crested waves the incident flows are purely two-dimensional, i.e. the flow velocity \underline{v} in the incident wave is everywhere parallel to the paper of New et al.(1985) Figure 7. This means that the matrix V is a 2x2 matrix (with coordinate directions taken, say, x horizontally in the direction of wave travel and z vertically upwards, following Rainey (1989)) which can be written in terms of just two unknowns a & b , thus:

$$\begin{bmatrix} a & b \\ b & -a \end{bmatrix}$$

The matrix is symmetric because the off-diagonal elements can be written in terms of the velocity potential ϕ thus:

$$\partial^2\phi / \partial x\partial z = \partial^2\phi / \partial z\partial x$$

The sum of the diagonal terms is zero because it can be written in terms of the velocity potential thus:

$$\partial^2\phi / \partial x^2 + \partial^2\phi / \partial z^2$$

which is zero by Laplace's equation (actually all that is required is the assumed incompressibility of the fluid, which requires that the gain in x -velocity in the x -direction must equal the loss in z -velocity in the z -direction).

The unknowns a & b can be determined to a good approximation by considering a frame of reference moving horizontally at a constant speed equal to the forward speed

of the vertical face of the breaking wave, which may be seen from Figure 7 (a) to be 0.0269 length units in 0.1 time units, i.e. 4.64 m in 0.420 seconds or 11 m/s. In this frame the horizontal velocity in our chosen area (particle 36) is zero (subtracting 11 m/s from the horizontal particle velocity figures given in Table 5, whose mean is to a good approximation also 11 m/s), and its vertical velocity is by coincidence 11 m/s (see Table 5; the position-based velocity figure is here clearly the more reliable, see Figure 7(a) in New et al.(1985). Figure 8(a) reveals the uncertainty in reading off velocities there, but confirms that when the horizontal velocity is 11 m/s or 2.69 units, the vertical velocity is also close to 2.69 units). The particle acceleration and velocity gradient are the same in this frame as in a stationary frame, so we can write:

$$\begin{bmatrix} 54 \\ -36 \end{bmatrix} = \begin{bmatrix} a & b \\ b & -a \end{bmatrix} \begin{bmatrix} 0 \\ 11 \end{bmatrix}$$

given that the flow on the front face of the wave will appear to a good approximation steady (the "surfer's view") in this moving reference frame, so that $\partial \underline{v} / \partial t = 0$. Hence:

$$a = 36/11 = 3.27; \quad b = 54/11 = 4.91$$

Finally we can deduce the local fluid acceleration $\underline{\dot{v}}$ in the original stationary reference frame (in which the velocity is 11 m/s both horizontally and vertically) by writing:

$$\begin{bmatrix} 54 \\ -36 \end{bmatrix} = \underline{\dot{v}} + \begin{bmatrix} 3.27 & 4.91 \\ 4.91 & -3.27 \end{bmatrix} \begin{bmatrix} 11 \\ 11 \end{bmatrix}$$

Hence:

$$\underline{\dot{v}} = \begin{bmatrix} -36 \\ -54 \end{bmatrix}$$

In other words $\underline{\dot{v}}$ is by coincidence the same magnitude (viz. $\sqrt{54 \times 54 + 36 \times 36} = 65$ m/s/s or 6.5g) as \underline{a} , but at right angles to it. The two vectors, together with the velocity vector \underline{v} (in a stationary frame) are shown for clarity in pictorial form, in Figure 1.

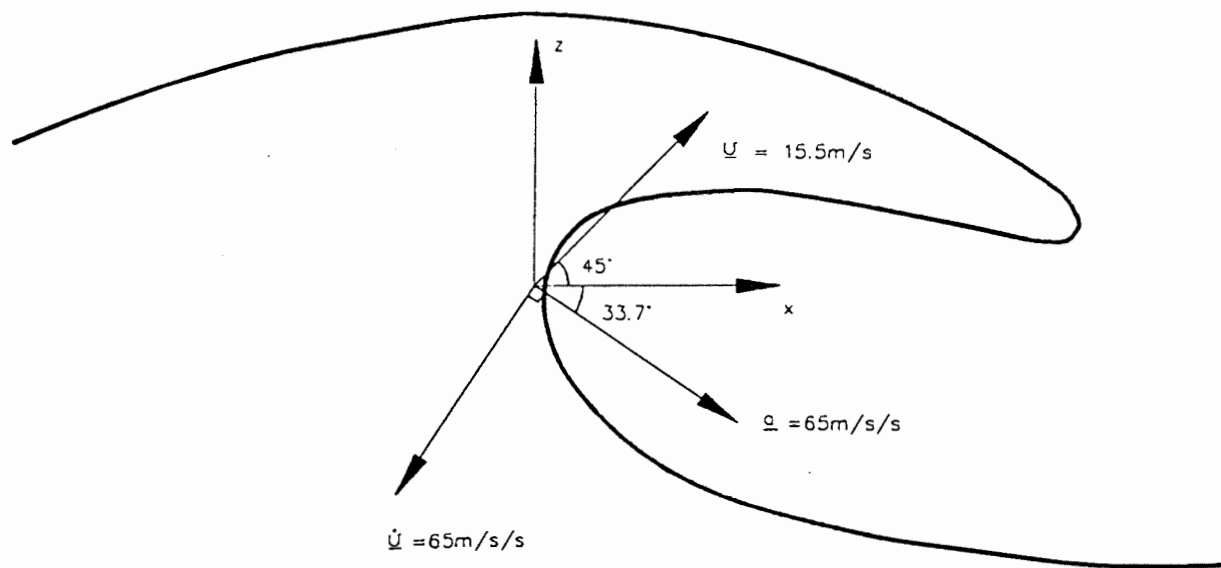


Figure 1: Fluid velocity \underline{U} , local acceleration $\underline{\dot{U}}$, and total acceleration \underline{a} , behind the vertical face of a breaking wave

2.4 Extent of high–acceleration region

Prof. Peregrine, the originator of the breaking wave data for New et al.(1985), has kindly provided printout from his computer program to complement Table 5. It is given in Tables 6 & 7, which give the horizontal and vertical fluid velocities at a grid of points behind the face of the wave, at the same instant in time as Table 5 (i.e. the instant when the wave has the profile shown in the last stage of Figure 7(a) in New et al. 1985). The grid shown spans the full vertical extent of the wave (28 points from -0.43 to $+0.38 = 0.81$ length units in all) but a comparatively small horizontal extent (10 points from 6.977 to $7.157 = 0.18$ length units in all). The position of the free surface is revealed by a sharp transition to the nominal velocity value of 1000, which is what the program prints when it encounters grid points in air rather than water. This transition can be clearly seen at the top left–hand corner of Tables 6 & 7 (it is highlighted there with a line), where it shows the back surface of the wave just behind the peak. Less clear is the transition at the front face of the wave, which is unfortunately blurred by numerical diffusion across the grid. Its position is however evident give or take one grid spacing, and has likewise been highlighted with a line, on the right of Tables 6 & 7.

To proceed further we must next interpret the non–dimensionalising scheme of Tables 6 & 7, which is different from that used by New et al.(1985) – this time the unit of length is wavelength/ 2π , although the unit of acceleration is still g. Thus, see 2.1, the unit of length is now:

$$172.73 / 2\pi = 27.49 \text{ m}$$

the unit of velocity is now:

$$41.164 / \sqrt{(2\pi)} = 16.42 \text{ m/s}$$

and the unit of time is now:

$$4.196 / \sqrt{(2\pi)} = 1.674 \text{ s}$$

A cross–check on these figures is the point in time specified in Tables 6 & 7, which is 3.890 or:

$$3.890 \times 1.674 = 6.512 \text{ s}$$

which agrees, as it should, with the time of 1.552 specified in New et al.(1985) p. 243 as corresponding to Table 5, which comes to:

$$1.552 \times 4.196 = 6.512 \text{ s}$$

identically.

Referring now to 2.3 above, the water velocity at our chosen point on the vertical face of the breaking wave is 11 m/s both horizontally and vertically, or in the new units:

$$11 / 16.42 = 0.670$$

This corresponds most closely to the point boxed in Tables 6 & 7, which is in the same position on the vertical wave face, and has horizontal and vertical velocities of 0.623 and 0.581 respectively. The resolution limitations of Tables 6 & 7 are however clearly seen – presumably the precise point is somewhat to the right (to bring the vertical velocity up to 0.670), and somewhat higher (to bring the horizontal velocity up to 0.670).

The next question is the velocity gradient, which as we saw in Section 2.3 here reduces to just two numbers: firstly the horizontal rate of change of horizontal velocity (equalling minus the vertical rate of change of vertical velocity and written a in Section 2.3), and secondly the horizontal rate of change of vertical velocity (equalling the vertical rate of change of horizontal velocity and written b in Section 2.3). Since our position on the

wave face gives us two alternative vertical increments in the grid of Tables 6 & 7 (1 up or 1 down) but just one horizontal increment (1 to the left), these tables yield three alternative estimates of each number in question.

Taking first a, the three are respectively:

$$\begin{array}{l} \text{---}(.3806\text{---}.5814)/.03 \text{ or } \text{---}(.5814\text{---}.4684)/.03 \quad \text{or } (.6234\text{---}.6087)/.02 \\ \text{i.e. } 6.69 \quad \text{or} \quad \text{---}3.77 \quad \text{or} \quad 0.735 \end{array}$$

The poor agreement here emphasises that the grid spacing is really too wide for our purposes: of the three figures most credence can be given to the first, since our desired data point is (see above) somewhat above and to the right of the grid point boxed in Tables 6 & 7. It compares with the figure of 3.27 /s derived in 2.3, which with our time unit of 1.674 s (see above) corresponds to a figure of $3.27 \times 1.674 = 5.47$. Turning now to b, the three alternative estimates are:

$$\begin{array}{l} (.8176\text{---}.6234)/.03 \quad \text{or} \quad (.6234\text{---}.4560)/.03 \text{ or } (.5814\text{---}.4355)/.02 \\ \text{i.e. } 6.47 \quad \text{or} \quad 5.58 \quad \text{or} \quad 7.30 \end{array}$$

which agree comparatively well, and compare with the figure derived in 2.3 which is 4.91/s or $4.91 \times 1.674 = 8.22$ in the present units.

These preliminary calibrations and cross-checks completed, we are now in a position to address the problem in hand, which is to estimate the extent of the high-acceleration region beneath the surface of the wave. The method used for the calculations in 2.3 was to adopt a frame of reference moving forward with the vertical wave face. In this frame, the flow appears steady and with near-zero horizontal velocity, so that the horizontal and vertical acceleration components are just the vertical velocity times b & a respectively. And we have just seen that b & a are proportional to the vertical velocity differences between (respectively) horizontally-neighbouring and vertically-neighbouring points in the grid. The whole picture can therefore be gauged by eye from Table 7 alone.

On the wave-surface, the horizontal and vertical acceleration components of 54 and 36 m/s/s quoted in 2.3 were (see above) the result of a vertical velocity of 0.670 in the present units, together with a vertical velocity difference of $8.22 \times .02 = 0.164$ between horizontally-neighbouring grid points, and coincidentally likewise $5.47 \times .03 = 0.164$ between vertically-neighbouring grid points. Examination of Table 7 shows that at two grid spacings in any direction from our reference point on the wave face, the vertical velocity has dropped to a little over a half of 0.670, and the velocity differences have dropped to a little under a half of 0.164, so that the water acceleration will have dropped by a factor of about 4.

Two grid spacings corresponds to a distance of $2 \times 0.02 \times 27.49 = 1.10$ m horizontally, and 1.65 m vertically. This relatively small extent of the region of extreme acceleration emphasises the idealised nature of the calculations in this report – in reality the members of jacket structures have cross-sections of a square metre or more, so that the acceleration will be by no means uniform around them, particularly in view of the disturbance they will make to the profile of the water surface as they pass through it. Such problems are however ignored in the standard wave loading calculation procedure, which deals solely in the water velocity and acceleration in the undisturbed wave at the point that would be occupied by the centreline of a structural member.

Table 6 : Horizontal fluid velocities at point behind face of the breaking wave

Variable: horizontal velocity. Time= 3.890, Depth= 0.4398, Gravity= 1.0000, Vorticity= 0.0000

x across	271	272	273	274	275	276	277	278	279	280		
y down	6.977	6.997	7.017	7.037	7.057	7.077	7.097	7.117	7.137	7.157		
28	0.380	1.000E+03	1.000E+03	1.000E+03	7.264E-01	7.469E-01	7.677E-01	7.887E-01	8.092E-01	8.301E-01	8.502E-01	28
27	0.350	6.653E-01	6.854E-01	7.061E-01	7.286E-01	7.517E-01	7.751E-01	7.987E-01	8.241E-01	8.482E-01	8.713E-01	27
26	0.320	6.604E-01	6.817E-01	7.038E-01	7.302E-01	7.559E-01	7.818E-01	8.081E-01	8.410E-01	8.682E-01	8.944E-01	26
25	0.290	6.538E-01	6.765E-01	6.985E-01	7.250E-01	7.551E-01	7.861E-01	8.177E-01	8.516E-01	8.875E-01	9.223E-01	25
24	0.260	6.395E-01	6.634E-01	6.894E-01	7.181E-01	7.499E-01	7.849E-01	8.232E-01	8.647E-01	9.084E-01	9.515E-01	24
23	0.230	6.223E-01	6.469E-01	6.738E-01	7.039E-01	7.378E-01	7.764E-01	8.204E-01	8.715E-01	9.305E-01	9.910E-01	23
22	0.200	6.010E-01	6.244E-01	6.509E-01	6.810E-01	7.157E-01	7.558E-01	8.021E-01	8.575E-01	9.354E-01	1.076E+00	22
21	0.170	5.738E-01	5.952E-01	6.196E-01	6.479E-01	6.814E-01	7.214E-01	7.677E-01	8.122E-01	8.244E-01	7.552E-01	21
20	0.140	5.413E-01	5.593E-01	5.797E-01	6.035E-01	6.322E-01	6.692E-01	7.231E-01	8.176E-01	9.360E-01	4.949E-01	20
19	0.110	5.047E-01	5.181E-01	5.327E-01	5.488E-01	5.667E-01	5.868E-01	6.087E-01	6.234E-01	3.915E-01	-4.062E-01	19
18	0.080	4.658E-01	4.740E-01	4.822E-01	4.899E-01	4.963E-01	4.991E-01	4.914E-01	4.560E-01	3.685E-01	2.424E-01	18
17	0.050	4.266E-01	4.300E-01	4.324E-01	4.334E-01	4.322E-01	4.285E-01	4.237E-01	4.291E-01	5.051E-01	1.327E+00	17
16	0.020	3.888E-01	3.881E-01	3.858E-01	3.841E-01	3.745E-01	3.644E-01	3.505E-01	3.293E-01	2.785E-01	1.123E-01	16
15	-0.010	3.536E-01	3.496E-01	3.436E-01	3.353E-01	3.240E-01	3.086E-01	2.875E-01	2.575E-01	2.150E-01	1.680E-01	15
14	-0.040	3.218E-01	3.152E-01	3.068E-01	2.959E-01	2.821E-01	2.647E-01	2.431E-01	2.170E-01	1.876E-01	1.591E-01	14
13	-0.070	2.935E-01	2.853E-01	2.752E-01	2.629E-01	2.481E-01	2.305E-01	2.099E-01	1.862E-01	1.591E-01	1.307E-01	13
12	-0.100	2.688E-01	2.595E-01	2.485E-01	2.356E-01	2.206E-01	2.033E-01	1.837E-01	1.616E-01	1.371E-01	1.099E-01	12
11	-0.130	2.476E-01	2.376E-01	2.261E-01	2.130E-01	1.982E-01	1.815E-01	1.629E-01	1.424E-01	1.200E-01	9.589E-02	11
10	-0.160	2.294E-01	2.191E-01	2.075E-01	1.944E-01	1.799E-01	1.640E-01	1.465E-01	1.275E-01	1.071E-01	8.547E-02	10
9	-0.190	2.140E-01	2.035E-01	1.919E-01	1.791E-01	1.651E-01	1.498E-01	1.334E-01	1.157E-01	9.702E-02	7.737E-02	9
8	-0.220	2.011E-01	1.906E-01	1.791E-01	1.666E-01	1.531E-01	1.385E-01	1.229E-01	1.064E-01	8.909E-02	7.101E-02	8
7	-0.250	1.903E-01	1.799E-01	1.686E-01	1.564E-01	1.433E-01	1.294E-01	1.146E-01	9.906E-02	8.283E-02	6.601E-02	7
6	-0.280	1.816E-01	1.712E-01	1.601E-01	1.482E-01	1.355E-01	1.221E-01	1.080E-01	9.326E-02	7.792E-02	6.209E-02	6
5	-0.310	1.746E-01	1.644E-01	1.534E-01	1.418E-01	1.295E-01	1.165E-01	1.029E-01	8.875E-02	7.412E-02	5.906E-02	5
4	-0.340	1.692E-01	1.591E-01	1.483E-01	1.369E-01	1.248E-01	1.122E-01	9.903E-02	8.536E-02	7.126E-02	5.680E-02	4
3	-0.370	1.653E-01	1.553E-01	1.446E-01	1.334E-01	1.215E-01	1.092E-01	9.628E-02	8.296E-02	6.924E-02	5.520E-02	3
2	-0.400	1.629E-01	1.529E-01	1.423E-01	1.311E-01	1.194E-01	1.072E-01	9.455E-02	8.145E-02	6.797E-02	5.419E-02	2
1	-0.430	1.618E-01	1.518E-01	1.412E-01	1.301E-01	1.185E-01	1.064E-01	9.378E-02	8.077E-02	6.741E-02	5.374E-02	1

Table 7 : Vertical fluid velocities at point behind face of the breaking wave

Variable: vertical velocity. Time= 3.890, Depth= 0.4398, Gravity= 1.0000, Vorticity= 0.0000

x across	271	272	273	274	275	276	277	278	279	280		
y down	6.977	6.997	7.017	7.037	7.057	7.077	7.097	7.117	7.137	7.157		
28	0.380	1.000E+03	1.000E+03	1.000E+03	-1.061E-01	-1.086E-01	-1.129E-01	-1.189E-01	-1.271E-01	-1.374E-01	-1.498E-01	28
27	0.350	-4.777E-02	-7.543E-02	-7.398E-02	-7.361E-02	-7.574E-02	-7.960E-02	-8.520E-02	-9.269E-02	-1.043E-01	-1.181E-01	27
26	0.320	-4.727E-02	-4.386E-02	-4.135E-02	-3.725E-02	-3.896E-02	-4.240E-02	-4.757E-02	-5.362E-02	-6.695E-02	-8.163E-02	26
25	0.290	-1.476E-02	-1.029E-02	-2.264E-03	4.186E-04	2.581E-03	3.783E-03	1.033E-03	-6.963E-03	-1.875E-02	-3.377E-02	25
24	0.260	1.855E-02	2.805E-02	3.681E-02	4.440E-02	5.060E-02	5.471E-02	5.542E-02	5.118E-02	4.038E-02	2.219E-02	24
23	0.230	5.306E-02	6.587E-02	7.869E-02	9.116E-02	1.029E-01	1.131E-01	1.210E-01	1.242E-01	1.178E-01	9.319E-02	23
22	0.200	8.691E-02	1.037E-01	1.213E-01	1.395E-01	1.581E-01	1.766E-01	1.951E-01	2.152E-01	2.391E-01	2.320E-01	22
21	0.170	1.187E-01	1.396E-01	1.623E-01	1.870E-01	2.137E-01	2.413E-01	2.678E-01	2.914E-01	3.382E-01	5.786E-01	21
20	0.140	1.466E-01	1.712E-01	1.987E-01	2.300E-01	2.659E-01	3.074E-01	3.531E-01	3.806E-01	2.188E-01	-5.717E-02	20
19	0.110	1.690E-01	1.960E-01	2.268E-01	2.626E-01	3.052E-01	3.590E-01	4.355E-01	5.814E-01	1.043E+00	1.758E-01	19
18	0.080	1.848E-01	2.127E-01	2.443E-01	2.806E-01	3.226E-01	3.713E-01	4.254E-01	4.684E-01	4.248E-01	1.976E-01	18
17	0.050	1.937E-01	2.210E-01	2.515E-01	2.858E-01	3.242E-01	3.665E-01	4.114E-01	4.564E-01	5.086E-01	5.578E-01	17
16	0.020	1.963E-01	2.220E-01	2.503E-01	2.815E-01	3.160E-01	3.545E-01	3.987E-01	4.546E-01	5.346E-01	5.884E-01	16
15	-0.010	1.937E-01	2.171E-01	2.424E-01	2.699E-01	2.996E-01	3.316E-01	3.588E-01	4.005E-01	4.286E-01	4.328E-01	15
14	-0.040	1.869E-01	2.077E-01	2.298E-01	2.532E-01	2.778E-01	3.033E-01	3.288E-01	3.529E-01	3.738E-01	3.917E-01	14
13	-0.070	1.771E-01	1.952E-01	2.141E-01	2.338E-01	2.540E-01	2.743E-01	2.943E-01	3.133E-01	3.311E-01	3.481E-01	13
12	-0.100	1.651E-01	1.807E-01	1.968E-01	2.132E-01	2.297E-01	2.461E-01	2.620E-01	2.771E-01	2.909E-01	3.031E-01	12
11	-0.130	1.517E-01	1.650E-01	1.786E-01	1.922E-01	2.058E-01	2.190E-01	2.317E-01	2.435E-01	2.541E-01	2.630E-01	11
10	-0.160	1.375E-01	1.488E-01	1.601E-01	1.714E-01	1.825E-01	1.933E-01	2.034E-01	2.127E-01	2.209E-01	2.277E-01	10
9	-0.190	1.228E-01	1.323E-01	1.417E-01	1.510E-01	1.601E-01	1.688E-01	1.769E-01	1.843E-01	1.907E-01	1.961E-01	9
8	-0.220	1.079E-01	1.158E-01	1.236E-01	1.312E-01	1.386E-01	1.456E-01	1.521E-01	1.580E-01	1.631E-01	1.673E-01	8
7	-0.250	9.294E-02	9.939E-02	1.058E-01	1.120E-01	1.179E-01	1.235E-01	1.287E-01	1.334E-01	1.374E-01	1.407E-01	7
6	-0.280	7.800E-02	8.321E-02	8.831E-02	9.326E-02	9.800E-02	1.024E-01	1.065E-01	1.102E-01	1.133E-01	1.159E-01	6
5	-0.310	6.315E-02	6.723E-02	7.121E-02	7.507E-02	7.873E-02	8.216E-02	8.529E-02	8.809E-02	9.051E-02	9.248E-02	5
4	-0.340	4.841E-02	5.145E-02	5.442E-02	5.728E-02	5.999E-02	6.252E-02	6.484E-02	6.689E-02	6.866E-02	7.011E-02	4
3	-0.370	3.376E-02	3.584E-02	3.787E-02	3.982E-02	4.167E-02	4.339E-02	4.495E-02	4.635E-02	4.754E-02	4.852E-02	3
2	-0.400	1.919E-02	2.036E-02	2.150E-02	2.259E-02	2.363E-02	2.459E-02	2.546E-02	2.624E-02	2.691E-02	2.746E-02	2
1	-0.430	4.662E-03	4.950E-03	5.229E-03	5.496E-03	5.749E-03	5.985E-03	6.199E-03	6.389E-03	6.552E-03	6.685E-03	1

3. DERIVATION OF WAVE LOADS: IMPROVING ON "MORISON'S EQUATION"

3.1 A general formula for the potential-flow load on a fixed cylinder in waves

This report is restricted to the case of fixed structures; we accordingly begin this Section by deriving from Rainey (1989) the formula for the potential-flow wave load-per-unit-length on a fixed cylinder in waves, on the assumption that its diameter is small compared with the wavelength. It is explained in the Introduction to Rainey(1989) that the wave load on such cylinders can be considered as the sum of the loading in potential (i.e. wake-free) flow, and the loading produced by the wake on its own. This is because the overall fluid velocity field around the cylinder is the sum of these two velocity fields, so that (loosely speaking) the overall rate-of-change of momentum is the sum of the rates-of-change of momentum in the two cases, and thus the overall fluid load is the sum of the fluid loads in the two cases (despite the fact that the overall fluid pressure is not the sum of the fluid pressures in the two cases).

In the case of uniform incident cross-flow (i.e. the conditions in a U-tube oscillating water column apparatus) it is easy to show that the original Morison inertia term (with $C_M = 2.0$ for a circular cylinder) gives the potential-flow load exactly, and that the drag term correctly corresponds to the loading from a wake with steadily-growing vorticity. In waves, however, the flow is non-uniform and it is known that, in general, the inertia term no longer gives the correct potential-flow load (even if it is based on total particle acceleration \underline{a} , as noted in Section 1), although the drag term is no less valid at describing the loading attributable to the wake. Hence the mathematical investigation of Rainey (1989), which derives the potential-flow load exactly, for the general case of a rigid lattice structure moving in waves.

To consider our case of a fixed structure, we will not set the structural velocity \underline{v} and angular velocity ω in Rainey (1989) to zero, but rather retain a steady translational velocity \underline{u} for the structure. This is a device automatically to check the consistency of the fluid loading formulae: if we switch to a frame of reference in which the structure appears to be moving in this way, the fluid loads should be unaltered. (The original Morison inertia term would incidentally fail this consistency test, because $\underline{\dot{v}}$ changes if a moving reference frame is adopted, see Section 2.3 above).

Considering a single fully-immersed finite-length cylinder translating in this way in waves, we see from equation 6.8 in Rainey (1989) (referring on to eqn. 5.13 for dI/dt , and to eqn. 6.9 for $\Delta e/\Delta X$) that the fluid load on the cylinder corresponds to a load-per-unit-length of:

$$M'(\underline{\dot{v}} + V\underline{u}) + VM'(\underline{v} - \underline{u})$$

where M' is the cylinder's added-mass-per-unit-length matrix (i.e. the matrix which sets axial vector components to zero, and multiplies transverse vector components by the 2-D added mass of the cylinder) plus the displaced-mass-of-fluid-per-unit-length, \underline{v} is the fluid velocity in the undisturbed wave, and V is the velocity gradient matrix (see 2.3 above). The reason that $(\underline{\dot{v}} + V\underline{u})$ appears in the first term, which is the one from the dI/dt term in eqn. 6.8, is that I is changing as a result of both fluid and structural velocity. The whole expression above can be rewritten:

$$\begin{aligned} & M'([\underline{\dot{v}} + V\underline{v}] - V[\underline{v} - \underline{u}]) + VM'(\underline{v} - \underline{u}) \\ &= M'\underline{a} + (VM' - M'V)(\underline{v} - \underline{u}) \end{aligned}$$

which is clearly unaltered, as it should be, if a moving reference-frame is chosen, because V and the particle acceleration \underline{a} are unaltered in a moving frame (see 2.3 above), and M' and the relative velocity $(\underline{v} - \underline{u})$ clearly are too.

In the above manipulations it is of course important to appreciate that the matrix products VM' and $M'V$ are not equal, as they would be if M' and V were scalars. For example, in the case of a vertical circular cylinder of circular cross-section c , and in the horizontal and vertical coordinate system of 2.3, the matrix M' is:

$$\begin{bmatrix} 2\rho c & 0 \\ 0 & \rho c \end{bmatrix}$$

where ρ is the density of water. Taking V as given in 2.3 in these coordinates we see that:

$$VM' = \begin{bmatrix} a & b \\ b & -a \end{bmatrix} \begin{bmatrix} 2\rho c & 0 \\ 0 & \rho c \end{bmatrix} = \begin{bmatrix} 2a\rho c & b\rho c \\ 2b\rho c & -a\rho c \end{bmatrix}$$

Whereas:

$$M'V = \begin{bmatrix} 2\rho c & 0 \\ 0 & \rho c \end{bmatrix} \begin{bmatrix} a & b \\ b & -a \end{bmatrix} = \begin{bmatrix} 2a\rho c & 2b\rho c \\ b\rho c & -a\rho c \end{bmatrix}$$

so that:

$$VM' - M'V = \begin{bmatrix} 0 & -b\rho c \\ b\rho c & 0 \end{bmatrix}$$

It is however possible to split out the part of M coming from the displaced-mass-of-fluid-per-unit-length, i.e. ρc , and write:

$$M' = M + \rho c$$

where M is the matrix of added mass on its own, which is in the above example:

$$\begin{bmatrix} \rho c & 0 \\ 0 & 0 \end{bmatrix}$$

In this manner $(VM' - M'V)$ can be written:

$$V(M + \rho c) - (M + \rho c)V = (VM - MV) + (V\rho c - \rho cV) = (VM - MV)$$

in which form it will be used below.

The expression for the fluid load above is complicated by the fact that it includes the fluid forces on the ends of the cylinders. The simplest of these is the axial end-force which is simply removed by taking the transverse component of the above expression, denoted henceforth by the subscript $(\)_T$. More subtle is the transverse fluid load at the cylinder ends (responsible e.g. for the "Munk moment" on cylinders moving obliquely in still water, see Section 3 in Rainey (1989)), which cannot be so readily separated out from the transverse fluid load distributed along the length of the cylinder. It is shown in Rainey (1989) (eqn. 7.7 supported by Section 7.1) that it can be removed by adding an equivalent transverse load per unit length of:

$$\mathbf{i} \cdot \nabla \{ [\mathbf{i} \cdot (\mathbf{v} - \mathbf{u})] M (\mathbf{v} - \mathbf{u}) \}$$

where \mathbf{i} is an axial unit vector. On differentiating term-by-term this becomes:

$$(\mathbf{i} \cdot \nabla) M (\mathbf{v} - \mathbf{u}) + [\mathbf{i} \cdot (\mathbf{v} - \mathbf{u})] M \nabla \mathbf{i}$$

$$= (\rho V)M(\underline{v} - \underline{u}) + MV([\underline{v} - \underline{u}] - [\underline{v} - \underline{u}]_T)$$

Thus in total the fluid load distributed over the length of the cylinder must be:

$$\begin{aligned} & \rho c \underline{a}_T + M\{\underline{a} + [V]\underline{v} - \underline{u}\} + [VM(\underline{v} - \underline{u})]_T - MV(\underline{v} - \underline{u})_T \\ = & \text{"Froude-Krilov"} + \text{"Added mass"} + \text{"VM"} + \text{"MV"} \end{aligned}$$

where we have collected the total effect of the displaced-mass part of M in a single "Froude-Krilov" term (with ρ denoting the water density and c the cylinder cross-sectional area, as before), and all the terms involving only the added mass matrix M in a single "added mass" term, which leaves two extra terms (which incidentally cancel each other out if the cylinder is circular, for then both equal $\rho c[V(v-u)]_T$), one involving only the matrix VM , and one only the matrix MV . It can readily be seen that all four terms are unaltered, as they should be, if a moving reference frame is taken.

3.2 First special case: cylinder parallel to wave crests

Probably the simplest case of fluid loading on a cylinder in waves is when the cylinder is parallel to the crests of unidirectional waves, because in this case alone the flow as a whole is two-dimensional i.e. the fluid velocity is everywhere parallel to the paper of Figure 7 in New et al.(1985). The above fluid loading formula reduces considerably, because V_i in the added mass term is zero, and the suffix $()_T$ can be omitted, so that the fluid load per unit length on a stationary cylinder can be written:

$$M'(\dot{\underline{v}} + V\underline{v}) + (VM - MV)\underline{v}$$

expanding \underline{a} in the manner of Section 2.3 above. Collecting terms this becomes:

$$\begin{aligned} & M'\dot{\underline{v}} + (M' - M)V\underline{v} + VM\underline{v} \\ = & M'\dot{\underline{v}} + VM'\underline{v} \end{aligned}$$

which is the expression derived by quite different means by Isaacson (1979) eqn. 17 (see also Rainey (1989) eqn. 7.5) and is a significant cross-check on the above algebra.

For the purposes of the calculations in Section 4 below we note here the further simplification possible in the special case of a circular cylinder, for which M is just a scalar in this two-dimensional problem, so that the fluid load per unit length becomes:

$$M'(\dot{\underline{v}} + V\underline{v}) = M'\underline{a}$$

as first observed by Isaacson (1979). It is effectively this one special-case result which has led to the standard procedure noted in Section 1, which is to replace $\dot{\underline{v}}$ in the original Morison inertia term with \underline{a} .

3.3 Second special case: circular cylinder perpendicular to the wave crests

The next simplest case is probably when the cylinder is perpendicular to the crests of unidirectional waves (i.e. vertical, horizontal in the direction of wave travel, or any angle in between), and is additionally circular (or slightly more generally has a principal axis of its added mass matrix perpendicular to the wave crests), for then the MV term in the loading formula in 3.1 above can be written:

$$- MV(\underline{v} - \underline{u})_{\tau} = - [VM(\underline{v} - \underline{u})]_{\tau}$$

which cancels with the VM term.

In addition, we can use the fact that the gradients in the incident flow occur only in the directions \underline{i} (along the cylinder) and \underline{j} (transverse to it, and perpendicular to the wave crests) to write:

$$\underline{i} \cdot \underline{V} \underline{i} + \underline{j} \cdot \underline{V} \underline{j} = 0$$

which is the condition that the sum of the diagonal elements in V are zero, as discussed in 2.3 above. Hence the $\underline{i} \cdot \underline{V} \underline{i}$ contribution to the added mass term in the loading formula in 3.1 above can be written for a stationary cylinder (for which \underline{j} is parallel to $M\underline{v}$):

$$- (\underline{j} \cdot \underline{V} \underline{j}) M\underline{v} = - (\underline{j} \cdot \underline{V} M\underline{v}) \underline{j} = - (VM\underline{v})_{\tau}$$

which is in fact minus the original VM term in the loading formula.

The total wave load can thus be written:

$$M'(\underline{a})_{\tau} - (VM\underline{v})_{\tau}$$

which is the load given by the Morison inertia term with \underline{a} substituted for $\underline{\dot{y}}$, as described in 3.2 above, plus this additional term $-(VM\underline{v})_{\tau}$. This is a convenient formula for use in the calculations in Section 4 below, and also allows a powerful cross-check on the above algebra, because it agrees as it should with a vertical-cylinder result derived by quite different means by Lighthill (1979). Lighthill considered the special case of regular deep-water waves analysed in a Stokes' expansion to second order in waveheight, in which situation the convective component of \underline{a} is purely vertical, so that there is no second-order load contribution from the $M'\underline{a}_{\tau}$ term above, and Lighthill's result for the second-order load reduces as it should just to the $-(VM\underline{v})_{\tau}$ term above, see Rainey (1989) eqn. 7.6.

4. RESULTS OF SAMPLE CALCULATIONS

4.1 Choice of cylinder orientations for analysis

In view of 3.2 and 3.3 above, the simplest series of fixed cylinder orientations to analyse are:

- 1) a circular cylinder parallel to the wave crests (using the theory of 3.2); and
- 2) circular cylinders perpendicular to the wave crests, but at a series of different angles to the vertical (using the theory of 3.3).

This is not precisely as envisaged at the start of this work, when it was thought that horizontal cylinders at various angles to the wave crests would be a suitable series for analysis. However, it is clear that (1) plus the series (2) is highly representative, as well as being simpler to handle algebraically and easier to describe pictorially. This is because the series (2) includes the both the extreme cases where the water velocity is axial with the cylinder, and where it is normal to it; and the same for the water acceleration. At the same time, the essential feature of horizontal cylinders which are not perpendicular to the wave crests is included, from case (1).

As for the cylinder radius, a nominal value of 1m is used. This is typical of the legs of the small jacket structures typically exposed to breaking waves. The relative proportions of all the potential-flow loads (and the Morison inertia term) are independent of cylinder diameter; their collective size compared with wake-induced loads (as described by the Morison drag term) is directly proportional to cylinder diameter. This means the results below read across without difficulty to all small cylinder diameters.

4.2 Potential-flow load

From 3.2 above, the potential-flow load on a circular cylinder parallel to the wave crests is simply $M'\underline{a}$, where for this case M' is the scalar $2\rho c$, or 2π tonnes/m for our 1m radius cylinder. This figure is shown in Figure 2.

From 3.3 above, the potential-flow load on a circular cylinder perpendicular to the wave crests has two components, firstly $M'(\underline{a})_{\perp}$ which is in our case $2\rho\pi(\underline{a})_{\perp}$ and is readily plotted from the sine of the angle between the cylinder and \underline{a} as shown in Figure 3, and secondly $-(VM\underline{v})_{\perp}$. If we write the angle of our cylinder to the vertical (measured anticlockwise in Figure 1; see Figure 3) as θ , then the normal to the cylinder in the x-z coordinate system of 2.3 is:

$$\begin{bmatrix} \cos \theta \\ \sin \theta \end{bmatrix}$$

and the normal component of our instantaneous value of \underline{v} (viz. 11 m/s in both x and z directions, see 2.3) is $11(\cos\theta + \sin\theta)$, so $M\underline{v}$ is evidently:

$$11\rho\pi(\cos\theta + \sin\theta) \begin{bmatrix} \cos \theta \\ \sin \theta \end{bmatrix}$$

Thus $VM\underline{v}$ is:

$$\begin{bmatrix} 3.27 & 4.91 \\ 4.91 & -3.27 \end{bmatrix} 11\rho\pi(\cos\theta + \sin\theta) \begin{bmatrix} \cos \theta \\ \sin \theta \end{bmatrix}$$

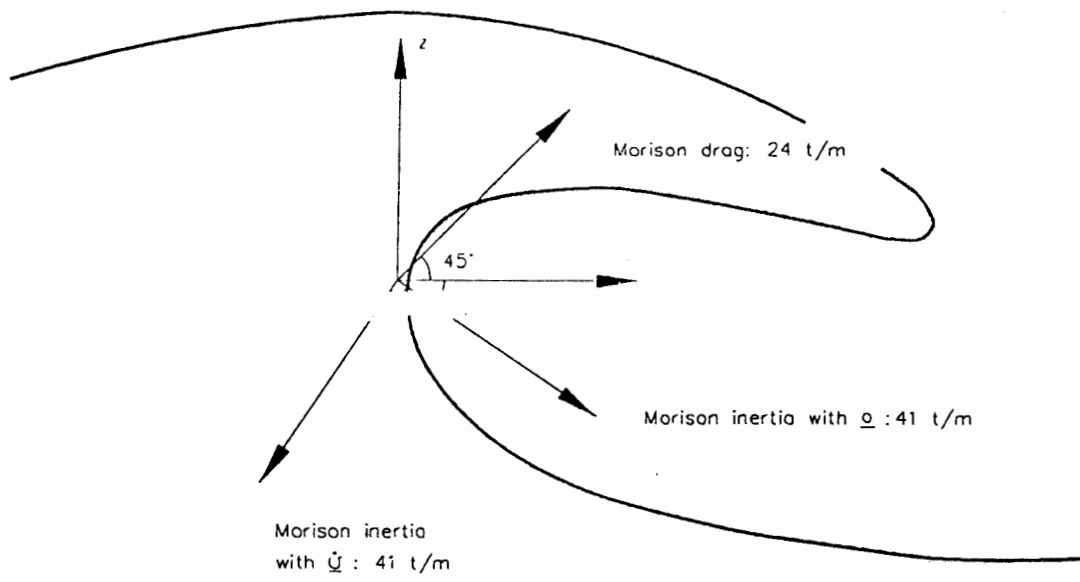


Figure 2: Loads on cylinder of 1 metre radius parallel to wave crest

$$= 11\rho\pi (\cos\theta + \sin\theta) \begin{bmatrix} 3.27\cos\theta + 4.91\sin\theta \\ 4.91\cos\theta - 3.27\sin\theta \end{bmatrix}$$

and $-(VM\underline{y})_{\tau}$ is given by taking (minus) the scalar product of this vector with the above cylinder normal, which gives the strength of the force $-(VM\underline{y})_{\tau}$ measured in the sense of that normal as:

$$\begin{aligned} & - 11\rho\pi (\cos\theta + \sin\theta)(3.27\cos^2\theta + 4.91\sin\theta\cos\theta + 4.91\cos\theta\sin\theta - 3.27\sin^2\theta) \\ = & - 11\rho\pi (\cos\theta + \sin\theta)(3.27[\cos^2\theta - \sin^2\theta] + 4.91[2\cos\theta \sin\theta]) \\ = & - 11\rho\pi (\cos\theta + \sin\theta)(3.27\cos 2\theta + 4.91\sin 2\theta) \end{aligned}$$

which is plotted in Figure 3.

4.3 Load from the original and modified Morison inertia term

The fluid load predicted by the original Morison inertia term (see e.g. Hallam et al. (1978) eqn. 4.61, and extensively above) can very readily be calculated from the information in 2.3. The load is obtained simply by taking the transverse component of $\underline{\dot{y}}$, which is $\underline{\dot{y}}$ itself for the cylinder parallel to the wavecrests, and otherwise can be obtained from the sine of the angle between $\underline{\dot{y}}$ and the cylinder; it shown in this way (with the potential-flow value for M' for consistency, corresponding to $C_M = 2$ in Morison's equation) in Figures 2 and 3.

In the standard modification of the Morison inertia term noted extensively above, $\underline{\dot{y}}$ is replaced by \underline{a} . This procedure gives the correct potential-flow load for a circular cylinder parallel to the wave crests, but not otherwise. It corresponds to the first part of the full potential-flow load calculated in 4.2 above, and is already shown in Figures 2 and 3.

4.4 Load from the Morison drag term

Finally the load-per-unit-length predicted by the Morison drag term is of the utmost relevance because as described in 3.1, it correspond to the additional load caused by the wake which, in theory, adds directly onto the potential-flow load.

It is obtained from the transverse component of the fluid velocity, which can be simply obtained as above, squared and multiplied by the water density and cylinder radius (this corresponds to a nominal Morison drag coefficient of 1, which is somewhat higher than the values typically used for design purposes, but is in line with values found experimentally). The result is plotted in Figures 2 and 3.

It should be remembered that the location within the wave and timing have been chosen for the maximum water particle acceleration (see 2.2 above), and do not correspond to the position and time where the fluid velocity is at its maximum. From Figure 8(a) in New et al.(1985) we see that this maximum velocity is approximately 30% higher than the velocity we have considered, which will give, depending on the orientation of the cylinder (maximum drag will occur at a different orientation, because the direction of the fluid velocity is different), drag forces up to 70% higher the maximum value shown in Figures 2 and 3.

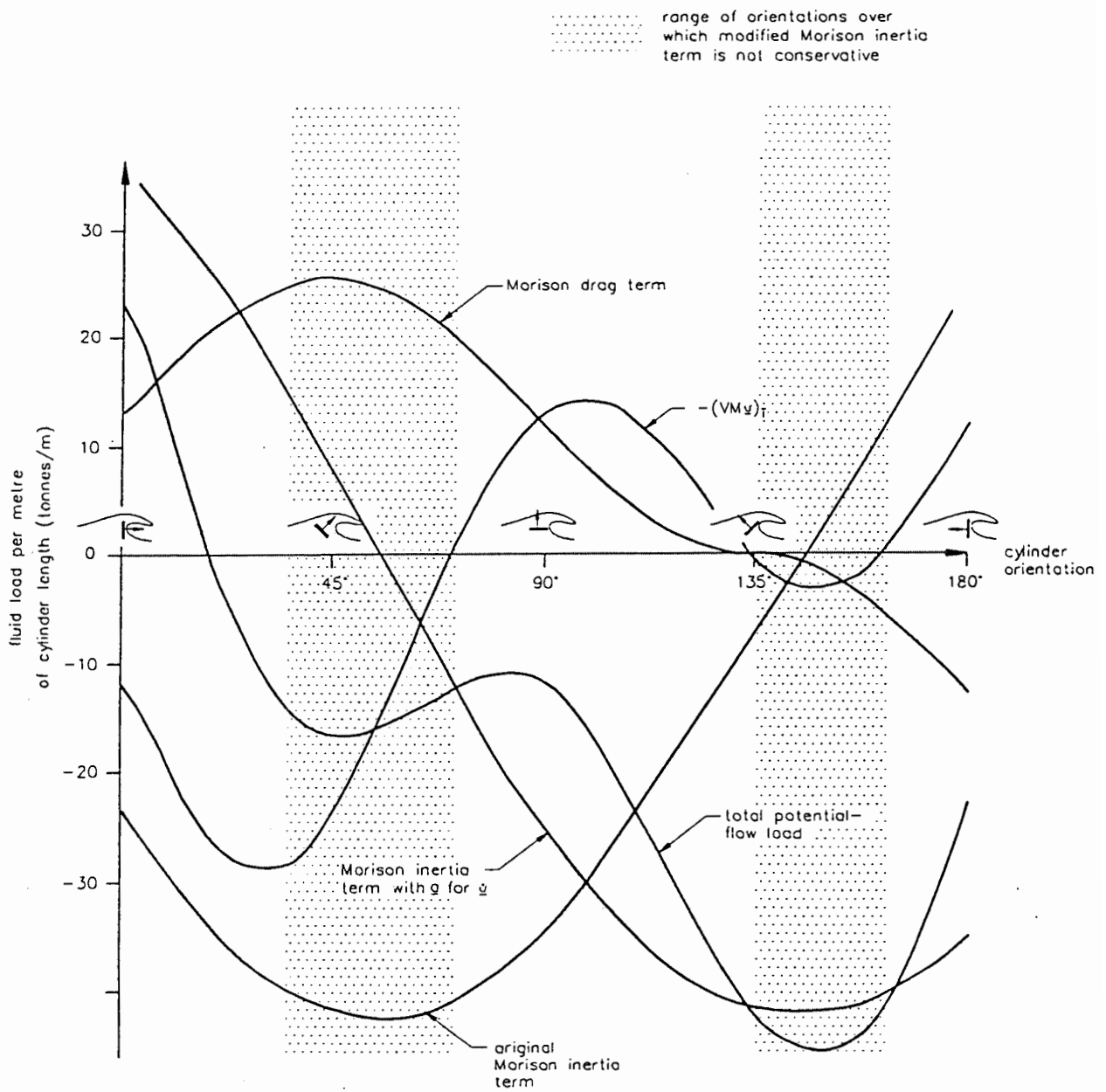


Figure 3: Wave loads on 1 metre radius cylinders of various orientations

5. CONCLUSIONS

The conclusions of this work are:

- For the 100-year design wave parameters typical of breaking-wave-prone areas of the North Sea, a breaking wave has comparable fluid velocities, but very much higher fluid accelerations, than a non-breaking wave. These high accelerations occur in a relatively small region behind the vertical part of the wave face.
- Standard practice is to calculate the fluid load from the fluid velocity and acceleration in the undisturbed wave at the point where the centreline of a structural member would be. Thus this high fluid acceleration will lead to large inertial fluid load estimates in that region of the wave, as high on 1m radius members as the velocity-induced drag loads on such members anywhere else in the wave. The ratio of these two types of load will (as usual) be directly proportional to cylinder diameter, larger diameters increasing the relative size of the inertial load. 1m radius is however typical of the legs of the small jacket structures in the relevant areas of the North Sea – evidently, therefore, these structures are not as totally "drag dominated" as is commonly supposed.
- The standard Morison term for calculating inertial loads is however not capable of accounting correctly for the large convective component of the water acceleration. When the convective component is ignored, as in the original Morison inertia term, it gives a very poor picture of the load from the fluid acceleration.
- The picture improves when the convective acceleration is included in the Morison inertia term, but this standard procedure is not always conservative (as is commonly supposed), significantly underestimating the inertial loads over a substantial range of structural member orientations. The most rigorous procedure is to adopt the exact potential-flow loading formula used in this report, as a direct replacement for the Morison inertia term.

REFERENCES

1. Bartrop, N.D.P., Mitchell, G.M. & Atkins, J.B. 1987 Fluid Loading on Fixed Offshore Structures – Background to a Proposed Revision of "Offshore Installations: Guidance on Design and Construction" Epsom: WS Atkins for the Department of Energy
2. Batchelor, G.K. 1967 An Introduction to Fluid Dynamics, 1st Ed. Cambridge: University Press
3. Hallam, M.G., Heaf, N.J. & Wootton, L.R. 1978 Dynamics of Marine Structures, 2nd Ed. London: CIRIA Underwater Engineering Group, Report UR 8
4. Isaacson, M.de St. Q 1979 J. Waterways etc. Div. Am. Soc. Civ. Eng. WW3, 213–227
5. Lighthill, Sir James 1979 Proc. 2nd Int. Conf. on the Behaviour of Offshore Structures, vol. 1, pp. 1–40. Cranfield: BHRA Fluid Engineering
6. New, A.L., McIver, P. and Peregrine, D.H. 1985 Computations of Overturning Waves. Journal of Fluid Mechanics vol. 150 pp. 233–251
7. Ochi, M.K. & Tsai, C–H 1984 Applied Ocean Research vol. 6, no. 3 157–165
8. Rainey, R.C.T. 1989 A New Equation for Calculating Wave Loads on Offshore Structures Journal of Fluid Mechanics vol. 204 pp 295–324.
9. Sarpkaya, T. & Isaacson, M. de St. Q. 1981 Mechanics of Wave Forces on Offshore Structures, New York: Van Nostrand Reinhold



HMSO publications are available from:

HMSO Publications Centre

(Mail and telephone orders only)
 PO Box 276, London SW8 5DT
 Telephone orders 071-873 9090
 General enquiries 071-873 0011
 (queuing system in operation for both numbers)

HMSO Bookshops

49 High Holborn, London WC1V 6HB 071-873 0011 (Counter service only)
 258 Broad Street, Birmingham B1 2HE 021-643 3740
 Southey House, 33 Wine Street, Bristol BS1 2BQ (0272) 264306
 9-21 Princess Street, Manchester M60 8AS 061-834 7201
 80 Chichester Street, Belfast BT1 4JY (0232) 238451
 71 Lothian Road, Edinburgh EH3 9AZ 031-228 4181

HMSO's Accredited Agents

(see Yellow Pages)

and through good booksellers

£26 net

ISBN 0-11-4 13316-6



9 780114 133160

